Academy of Sciences of the Czech Republic
Institute of Organic Chemistry and Biochemistry
Center for Biomolecules and Complex Molecular Systems

and

Charles University, Faculty of Science
Department of Physical and Macromolecular Chemistry

Theoretical Study of Ions at Phase Interfaces

Doctoral Thesis

Prague 2007

RNDr. Luboš Vrbka

Akademie věd České republiky
Ústav organické chemie a biochemie
Centrum biomolekul a komplexních molekulových systémů

a

Přírodovědecká fakulta Univerzity Karlovy v Praze
Katedra fyzikální a makromolekulární chemie

Teoretická studie iontů na fázových rozhraních

Disertační práce

Praha 2007

RNDr. Luboš Vrbka

To Sisa

Firstly I would like express my deepest love to Sisa and thank her for constant support, patience, and understanding.

My advisors, Pavel Jungwirth and Petr Nachtigall, guided me through new realms of the vast land of computational chemistry and made almost four years of my doctoral studies a really enjoyable experience.

This work would not exist without help coming from my family. I really appreciate it very much. My friends Detlef and Rosa also helped me a lot.

Supercomputer Centre Brno is acknowledged for continuous technical support and providing their computer facilities that were used to carry out the research reported in this work.

And last but not least, big thanks go to my colleagues from the Center for Biomolecules and Complex Molecular Systems – to Babak, Basia, Jirka, Lukasz, Martin, Robert, Tereza, and Zuzka – for creating a harmonious (not only) working atmosphere.

I solemnly swear that I wrote this thesis myself and that it represents the results of my own work, unless stated otherwise in the text. All books, articles, internet sites, and other sources of information used are properly cited in the References section.

Neither the thesis nor any of its parts have been used previously for obtaining any academic degree.

Luboš Vrbka

Contents

List of Figures

List of Abbreviations

BPTI	bovine pancreatic trypsin inhibitor
BSA	bovine serum albumine
DFT	density functional theory
DMP	1-dodecyl-4-(dimethylamino)pyridinium
DPN	2-[4-(dimethylamino)pyridinio]dodecanoate
HRP	horseradish peroxidase
MD	molecular dynamics
PBC	periodic boundary conditions
RNase A	ribonuclease A
QM	quantum mechanics
SHG	second harmonic generation
SFG	sum frequency generation
SPC/E	simple point charge extended water model
TAA	tetraalkylammonium
TBA	tetrabutylammonium
TEA	tetraethylammonium
TMA	tetramethylammonium
TPA	tetrapropylammonium
VSFG	vibrational sum frequency generation

Preface

Aqueous ionic solutions and their interfaces play a very important role in many natural and technological processes. To mention just a few examples, ions at the air/water interface are important for atmospheric chemistry taking place on ocean surface and seawater aerosols.[1,2] Brine rejection, involving the seawater/ice interface has far reaching consequences for the global climate.[3] Technologically important corrosion processes occur at the electrolyte/metal interfaces.[4] Protein stability and function can be largely affected by ions present at the biomolecule/solution interfaces.[5] Formation and stability of colloidal aggregates (vesicles, micelles) is also influenced by the presence of ions.[6] Metal cations and proton on the solid-gas and solid-liquid interfaces show unique sorption and catalytic properties. Cations on the internal (solid) surface of zeolites and related molecular sieves are essential in numerous technological applications, including catalysis, energy/gas storage, gas separation, or ion exchange.[7]

The present work focuses on three different topics, with ionic behavior at interfaces being the common denominator. Namely, we studied the behavior of various ions at the air/water interface (study of solvation properties of simple tetraalkylammonium cations, benzene dicarboxylate dianions, and ionic and zwitterionic surfactants), at the ice/water interface (study of brine rejection from freezing salt solutions), and at the protein/water interface (study of the effect of salts on the enzymatic activity of horseradish peroxidase, and of preferential adsorption of cations to protein surfaces). This thesis consists of 10 publications[8–17] and is divided into three parts. Each type of interface is presented with an extended introduction and a detailed discussion of results presented in the scientific journals.

The results behind this thesis were obtained using the methods of computational chemistry. Due to fast development in the computer industry and science, computer simulations are becoming more and more affordable way of getting relevant information, usually not available from conventional experimental techniques. Simulations can also serve as a valuable tool in the interpretation of experimental data. Examples of such cooperation are present also in this thesis where, *e.g.*, our calculations allowed for better understanding of photoelectron spectra of aqueous salt solutions[8,9,14] (see Chapter 2 for detailed discussion).

Chapter 1 briefly discusses the methodology used in our studies – molecular dynamics – together with some problems pertinent to the simulations of interfaces. Our studies of ions at the air/water, ice/water, and protein/water interfaces are discussed separately in

Chapters 2, 3, and 4. The summary and conclusions are given in Chapter 5. All articles constituting this thesis are given as Appendices. Note that the publications are attached only in the manuscript version. Due to copyright issues, the online version does not contain the articles. The reprints are, however, available upon request.

Chapter 1

Molecular dynamics

Most of the calculations pertinent to this work were performed using *molecular dynamics* (MD) simulations. Some important concepts and terms related to this method are discussed and explained in this chapter. The theory behind the method is described in detail in several computational chemistry textbooks.[18-20]

1.1 Molecular mechanics

Many of the problems solved by computational chemistry concern systems which are too large for quantum mechanical methods that explicitly consider electrons. The calculations can easily become computationally prohibitive due to the amount of required resources (CPU time, memory and harddrive storage). The basic idea of *molecular mechanics*, called also the empirical potential model, is that the total energy is given solely by the potential energy V of the atomic nuclei, *i.e.*, as a function of nuclear positions.

The molecular mechanics is based upon a simple model. The total energy of the system V is calculated from contributions corresponding to bond stretching, angle bending, bond rotation, and intermolecular terms, as indicated in the following equation.

$$V = \underbrace{\underbrace{\sum_{BONDS} E_i^{STRETCH} + \sum_{ANGLES} E_i^{BEND} + \sum_{TORSIONS} E_i^{TORSION}}_{BONDED} + \underbrace{\sum_{i<j} E_{i,j}^{VDW} + \sum_{i<j} E_{i,j}^{EL}}_{NONBONDED} + \ldots}_{} \tag{1.1}$$

The energy values arise from deviation of bonds and angles from their optimal values (bonded terms) and from non-bonded interactions (van der Waals, Coulombic, ...). The actual implementation of such approach is called a *force field*. The *force field parameters*

are used for a description of the behavior and properties of the system. These parameters include the optimal values, but also force constants, information on energy barriers of rotation about single bonds, and intermolecular parameters.

Bonded terms

The typical examples of the bonded terms are bond stretching, angle bending, and torsional/dihedral angle rotation.

$E^{STRETCH}$ corresponds to bond stretching. It can be defined as

$$E_i^{STRETCH} = \frac{k_i}{2}(l_i - l_{i,0})^2 \tag{1.2}$$

where k_i is a constant defining the force needed to stretch the bond, $l_{i,0}$ is an ideal bond length and l_i is the length of the stretched bond. This functional form (harmonic potential) does not allow for bond dissociation to occur. For processes related to bond dissociation and formation the Morse potential introduced in 1929[21] can be used instead.

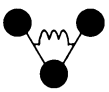

E^{BEND} models the valence angle bending. Valence angle is the angle A-B-C, where A and C are both bound to B.

$$E_i^{BEND} = \frac{k_i}{2}(\Theta_i - \Theta_{i,0})^2 \tag{1.3}$$

In this equation, k_i is a constant defining the force needed to bend the angle, $\Theta_{i,0}$ is the optimal value, and Θ_i is the actual value of the angle.

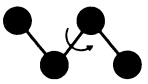

$E^{TORSION}$ assumes the energy of rotation around single bonds and the interactions between the substituents on the neighbouring atoms affected by this rotation.

$$E_i^{TORSION} = \frac{V_n}{2}(1 + \cos(n\omega_i - \omega_{i,0})) \tag{1.4}$$

V_n is a constant defining the energy needed to rotate around the n-fold rotation axis, $\omega_{i,0}$ is the optimal value of the dihedral angle, and ω_i is its actual value.

The *torsional angle* A-B-C-D is defined as angle between planes A-B-C and B-C-D. The term *dihedral angle*, which is used commonly instead of the torsional angle, is defined as angle between the normal vectors of planes A-B-C and B-C-D.

Nonbonded terms

Two basic examples of nonbonded interactions are long–range electrostatic (Coulombic) forces and short–range dispersion (van der Waals) forces.


The energy of the *electrostatic interactions* is calculated using the E^{EL} term based on the *Coulomb law.*

$$E_{i,j}^{EL} = \frac{q_i q_j}{4\pi\varepsilon_0 R_{ij}} \tag{1.5}$$

Charges of the atoms i and j are denoted q_i and q_j, R_{ij} is their distance and ε_0 is the permitivity of vacuum.


The E^{VDW} term is used to calculate energy of the *van der Waals interactions.*

$$E_{i,j}^{VDW} = \frac{A_{ij}}{R_{ij}^{12}} - \frac{B_{ij}}{R_{ij}^{6}} \tag{1.6}$$

The values A_{ij} and B_{ij} are constants characterizing the type and intensity of the interaction of this type between atoms i and j, R_{ij} is their distance. This is an example of the so-called *6/12 potential* called also *Lennard-Jones potential.* Other potentials are also defined (for example the *10/12 potential* is frequently used for the description of hydrogen bonds).

The force field does not necessarily include all the terms mentioned in Equation 1.1. It can of course contain some additional terms; also the method to compute a particular contribution may differ according to the force field definition and purpose.

1.2 Molecular dynamics

Molecular dynamics is a simulation method providing dynamical data obtained from the computer evaluation of intra- and intermolecular forces between all particles in the system. These forces are usually calculated using the molecular mechanics model (see page 12). The configurations of the system are generated by integrating the Newton's equation of motion

$$\frac{d^2\vec{r}_i}{dt^2} = \frac{\vec{F}_i(\vec{r}_1, \vec{r}_2, \ldots, \vec{r}_N)}{m_i} \tag{1.7}$$

where

$$\vec{F}_i = -\nabla_i V(\vec{r}_1, \vec{r}_2, \ldots, \vec{r}_N) \tag{1.8}$$

and

$$\nabla_i = \left(\frac{\partial}{\partial x_i}; \frac{\partial}{\partial y_i}; \frac{\partial}{\partial z_i}\right)$$

These equations describe the motion of a particle of mass m_i and position $\vec{r}_i$. The force $\vec{F}_i$ acting on the particle i (*i.e.*, the direction and magnitude of the force) is given by the potential energy gradient $-\nabla_i V$. The result of such simulation is called a *trajectory.* It represents the evolution (variance in positions and velocities of particles) of the simulated system in time.

Selecting the length of the integration step is a crucial point in the setup of any MD simulation. Its length has to be short enough to be able to precisely describe vibration of bonds. In case the time step is too short the calculation is very slow and ineffective. On the other hand a step too large introduces numerical instability into the algorithm.

1.3 Polarization interaction

For some MD simulations it is crucial to include the treatment of the polarization interaction in the forcefield. Theoretical study of structure and dynamic of ions at the air/water interface that will be discussed in more detail in Chapter 2 serves as a good example.

The atomic, ionic, or molecular *polarizability* represents the ability to undergo electronic polarization – displacement of the electronic cloud with respect to nuclear coordinates – under the influence of an external electric field. The response to an external electric field is given by

$$\vec{p} = \overleftrightarrow{\alpha}\, \vec{E} \tag{1.9}$$

i.e., the induced dipole $\vec{p}$ is linearly dependent on the polarizability $\overleftrightarrow{\alpha}$ and electric field $\vec{E}$. In the MD simulations, each atomic site i is typically assigned an isotropic polarizability α_i. Eqn. 1.9 can be then rewritten as

$$\vec{p_i} = \alpha_i \vec{E_i} \tag{1.10}$$

The atomic site i experiences the total electric field $\vec{E_i}$ dependent on all other charges and induced dipoles in the system

$$\vec{E_i} = \vec{E_i^C} + \sum_{j \neq i} \vec{T_{ij}} \vec{p_j} \tag{1.11}$$

$\vec{E_i^C}$ corresponds to the electric field due to charge distribution in the system and $\vec{T}$ to the dipole–dipole interaction tensor.

The set of equations for all atomic sites has to be solved iteratively. As a first guess, the values from the previous simulation step are used, assuming that neither component of the total electric field changes significantly.

For highly polarizable species (*e.g.*, molecular anions like sulfate, azide, or thiocyanate), this approach can easily lead to the so called *polarization catastrophe.*[22] When two atomic sites get closer than some critical distance, the induced dipoles diverge, yielding an infinite negative energy. This critical distance is dependent on the value of polarizability, being larger for more polarizable species.

A possible scheme for treating this problem was developed by Mucha.[23,24] Its principle is depicted in Fig. 1.1. The dependence of the induced dipole on the electric field is linear only in the limit of small fields. Above a cetrain field strength the induced dipole levels off, avoiding thus the problem of polarization catastrophy.

1.4 Periodic boundary conditions

The aim of MD simulations is to provide information about macroscopic systems. However, with current computer technology, number of particles that can be conveniently handled

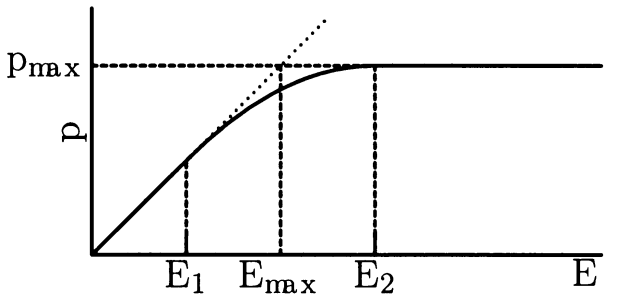

Figure 1.1: Dependence of size of induced dipole p on the electric field strength E. Figure adopted with permission from Ref.[23].

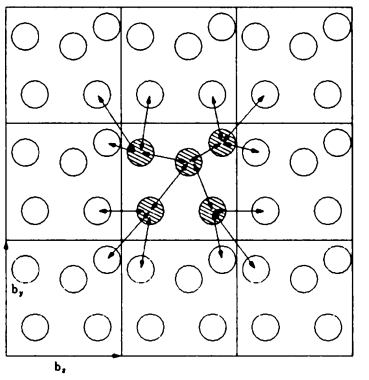

Figure 1.2: Periodic boundary conditions. 'Particles' in the central box are shaded.

ranges from several hundreds to millions. Even for the latter it is evident that the number is still far from reality.

In order to simulate bulk phases (liquid, solid) it is, therefore, necessary to employ appropriate boundary conditions. This task is usually achieved by using periodic boundary conditions (PBC, see Figure 1.2). The simulation box is treated as a unit cell in an infinite periodic lattice. Then, each particle interacts with others in the unit cell, as well as with all periodic images (including its own images).

1.4.1 Slab geometry

The use of periodic boundary conditions is perfectly appropriate for simulations of bulk systems, that uniformly fill the whole volume of the simulation cell. However, a different approach has to be adopted for calculations involving air/water interfaces. In such, a cubic unit cell is extended along a selected axis (*e.g.*, z-axis, see Figure 1.3). In other two directions, the cell remains unchanged. Replication of the simulation box along these two unchanged axes (2D periodic boundary conditions) leads to formation of extended slab with two interfaces.

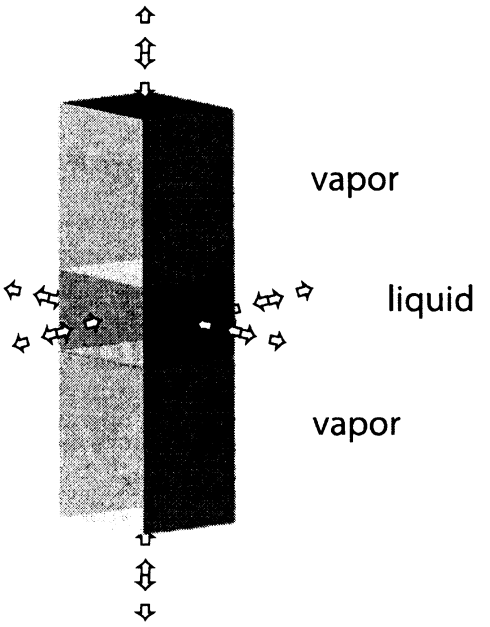

Figure 1.3: Slab periodic boundary conditions. Original water unit cell is elongated in the z–direction to create two air/water interfaces. After applying 3D PBC, set of extended water slabs separated by vacuum region is created.

For practical reasons, the unit cell is usually replicated in all 3 directions (3D periodic boundary conditions), forming infinite set of slabs in z-direction, separated by vacuum region. When a translationally hot molecule evaporates from the interface and leaves the upper side of the cell, it reappears from the bottom, preserving thus the number of particles in the simulation box. Moreover, the algorithm for treatment of long–range electrostatic interactions – Ewald summation[18,25–27] – is computationally efficient only in the 3D case.[28]

This, however, can bring an artifact to the simulation – an unrealistic interaction between the slabs. To avoid this interaction, two possibilities exist. First, it is possible to increase the separation between individual replicas of the slab by increasing the z–dimension of the simulation cell. Second, there is a possibility to use a slab correction proposed by Berkowitz and coworkers.[29] An extra term is used to introduce a force acting against the formation of nonzero z-component of the total dipole moment of the unit cell.

Chapter 2

Study of structure and dynamics of ions at the air/water interface

2.1 Introduction

First studies of the interfaces of aqueous salt solutions appeared in the beginning of the 20^{th} century. The experimentally observed increase of the surface tension of water after addition of salt was addressed by Wagner, Onsager and Samaras.[30,31] The increase was rationalized in terms of depletion of ions from the interface. This view (despite the fact that it did not take the ion specificity into account) has been widely accepted up until recently.

In 1990s the advance in computer technology allowed for a more detailed theoretical study of these phenomena. Namely, MD simulations of aqueous slabs indicated that certain inorganic ions show a propensity for the interface.[2,32–34] This prediction was also confirmed by the new surface-sensitive techniques such as second harmonic generation spectroscopy (SHG), vibrational sum-frequency generation spectroscopy (VSFG), or photoelectron spectroscopy (PES) in liquid jets.[8,35,36] The currently accepted picture is that large and polarizable ions show an appreciable propensity for the interface, whereas small and non-polarizable ions are repelled from the air/water interface (consistently with the classical picture).[34,37]

The first calculations that predicted the asymmetric (surface) solvation of certain atomic ions were simulations of clusters.[38–42] It was shown that the key point in these calculations was the use of polarizable potential models.[38] These predictions of asymmetric cluster solvation were confirmed by various experimental techniques[43,44] as well as electronic structure calculations, ab–initio molecular dynamics, and Monte Carlo simulations.[45–47] Asymmetric solvation was later predicted theoretically and supported experimentally (by photoelectron spectroscopy) also for soft molecular anions like azide and nitrate.[48,49]

The transferability of results from cluster surfaces to extended surfaces is somewhat ques-

tionable due to the finite size and surface curvature of the former.[50] Therefore, extending the work to larger systems was necessary. The pioneering simulations of single ions in aqueous slabs did not show any propensity of ions for the air/water interface.[32,33] This was partially due to the particular ions chosen (small hard ions, with the exception of chloride) and also due to the neglect of polarization interactions.

The first slab simulations of polarizable ions at the air/water interface appeared around the turn of the millenium, changing considerably the currently accepted picture.[2,51] Polarizable chloride anion was shown to weakly prefer surface solvation. An increasing surface propensity for heavier halides was also predicted.[52] Recently, similar surface enhancement of molecular anions was observed for azide and nitrate in a water slab.[48,49] Another molecular anion, sulfate, was found to prefer bulk solvation, mainly due to its double negative charge.[53] A more detailed overview of the topic can be found in a recent review article.[37]

The present work is a continuation and extension of these poioneering studies and is done in close collaboration with leading experimental laboratories, therefore, our results are validated using different spectroscopic techniques. We are also able to provide insight for systems that are currently hard to treat experimentally.

2.2 Summary of results

This chapter discusses and summarizes results of our work in the field of molecular simulations of molecular ions at the air/water interface. In the first paper[10] (Section 2.2.1), we summarize the reasons behind the fact that some ions can exhibit propensity for the interface. Solvation and interfacial properties of tetrabutylammonium cation with various counter–ions are studied in three publications (Sections 2.2.2, 2.2.3, and 2.2.4).[8,9,11] Our interest in interactions of proteins with ions, discussed in another article[17] (see Section 4.2.1), resulted in the study of the behavior of these biologically relevant species at the air/water interface (Section 2.2.5).[12] The following publication,[13] summarized in Section 2.2.6, is devoted to the theoretical study of zwitterionic and ionic surfactant molecules. A study of solvation properties of benzene dicarboxylate dianions and their methylated analogues is discussed in Section 2.2.7.[14]

2.2.1 Propensity of soft ions for the air/water interface

This article[10] discusses and rationalizes the fact that contrary to the classically accepted picture, certain ions can be present at the air/water interface.

One of the first experimental studies related to interfacial properties of electrolyte solutions is due to Heydweiller. In the beginning of the 20^{th} century, he carried out series of surface tension measurements of such solutions.[54] He found that adding salt resulted in an increase of surface tension. Cations exhibited low specificity. For anions, the behavior varied

depending on the nature of the ion and could be correlated with the Hofmeister series.[55] Strongly hydrated (kosmotropic) ions were found to raise the surface tension more than weakly hydrated (chaotropic) ions.

This behavior was addressed by Wagner, Onsager, and Samaras[30,31] in terms of the Gibbs adsorption isotherm.[56] In a two–phase system (air, water with interface area σ) containing additional components X, it is possible to define the so called surface excess as follows. In case that a component is distributed uniformly throughout the system, its total amount is given by the sum of respective amounts in both phases.

$$n_X = n_{X,air} + n_{X,water} \tag{2.1}$$

However, when the solute accumulates at the interface, the sum differs from the total amount by $n_X(\sigma)$.

$$n_X(\sigma) = n_X - [n_{X,air} + n_{X,water}] \tag{2.2}$$

The *surface excess* Γ_X of the component X is defined as

$$\Gamma_X = \frac{n_X(\sigma)}{\sigma} \tag{2.3}$$

where σ is the surface area. Surface excess can be positive (accumulation of X at the interface) or negative (depletion of X from the interface). The *Gibbs adsorption isotherm*[56] then reads

$$d\gamma = -\sum_X \Gamma_X d\mu_X \tag{2.4}$$

where the sum runs over all components, including water. Change in the surface tension $d\gamma$ is given by the composition of the surface, expressed as surface excess Γ_X of the component X and the differential of the chemical potential $d\mu_X$ of this component. A geometrically flat interface can be defined such that the surface excess of water is zero (the so called *Gibbs dividing surface*). If there is only one solute S, Eqn. 2.4 can be rewritten in the following form:

$$d\gamma = -\Gamma_S d\mu_S \tag{2.5}$$

An analogous equation can be derived for strong electrolyte solutions due to the condition of surface neutrality. In dilute solutions with the condition of constant temperature T, Eqn. 2.5 can be rearranged into

$$\left(\frac{\partial\gamma}{\partial \ln c}\right)_T = -RT\Gamma_S \tag{2.6}$$

This directly shows that the experimentally observed increase of the surface tension with salt concentration is caused by a negative surface excess of ions.

The question remains how it is possible to obtain a negative surface excess while having ions present at the interface. The definition of the surface excess (Eqn. 2.3) can be rewritten in terms of the ion density profile (distribution of ions across the interface) $\rho(z)$

$$\Gamma = \int_{-\infty}^{\infty} \rho(z)dz - \rho_{liq}\int_{z_{Gibbs}}^{\infty} dz - \rho_{gas}\int_{-\infty}^{z_{Gibbs}} dz \tag{2.7}$$

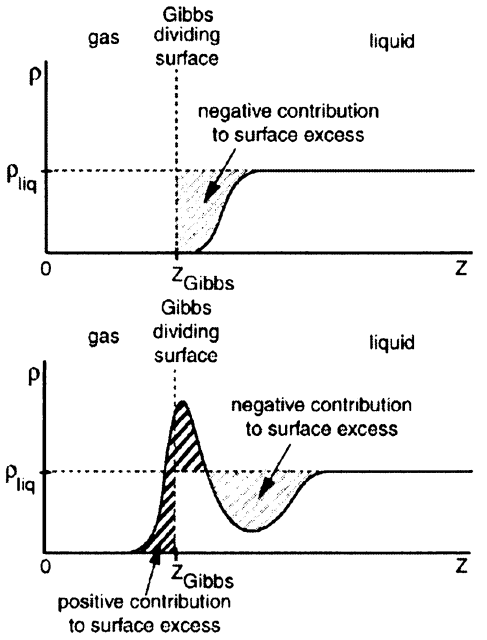

Figure 2.1: Two possibilities for obtaining a negative surface excess

where ρ_{liq} and ρ_{gas} are ion concentrations in the two phases. The ion density in the air phase is zero, therefore, it is possible to rearrange Equation 2.7 into

$$\Gamma = \int_{-\infty}^{z_{Gibbs}} \rho(z)dz + \int_{z_{Gibbs}}^{\infty} [\rho(z) - \rho_{liq}]\, dz \tag{2.8}$$

The situation is depicted in Figure 2.1. In the first case, the classical picture of obtaining negative surface excess (ions repelled from the interface) is displayed. In the second case, the surface enhancement of ion is accompanied by a subsurface depletion, providing together a negative surface excess. It is, therefore, demonstrated that the increase in surface tension does not rule out the presence of solute at the interface as long as the subsurface depletion is larger than the surface enhancement.

As was discussed in the introductory part of this chapter, the way to observe enhancement of certain ions at the air/water interface is via using a polarizable force field. When ion is brought to the interface, it has to overcome the desolvation energetic penalty. For polarizable ions this penalty can be overcome by the polarization stabilization, which is larger at the surface than in the bulk. Therefore, the more polarizable the ion is, the higher propensity for the interface.

In the article, it is also shown that polarization of both ions and water plays an important role. Another effect influencing the interfacial properties of ion is its size. Preference for the interface for larger ions is higher. Larger ions disrupt more the hydrogen bonded network in water and have thus a more hydrophobic character.

Another class of ions mentioned in this work and discussed in greater detail in our publications[8,9,11,12] (see Sections 2.2.2 to 2.2.5) are tetraalkylammonium (TAA) cations. For these ions it is mainly their hydrophobicity that drives them to the interface. From this perspective, the use of polarizable potential is, therefore, not crucial for strongly hydrophobic ions. However, counteranions that are present in the simulation cell to make it electrically neutral influence the distribution of cations (and vice versa). Employing a polarizable force field in the simulation may be therefore needed to obtain a correct description of counter–ions.

In summary, the article shows that molecular dynamics simulations indicate a strong specificity in the propensity of ions for the air/water interface. Small, nonpolarizable (hard) ions are repelled from the interface, consistently with the classical picture. Large, polarizable (soft) ions, however, have an appreciable affinity for the interface which correlates with their polarizability and size.

2.2.2 Molecular structure of surface-active salt solutions: Photoelectron spectroscopy and molecular dynamics simulations of aqueous tetrabutylammonium iodide

This study[8] was concerned with the molecular structure of the surface region of the aqueous solution of tetrabutylammonium iodide (TBAI). Tetrabutylammonium (TBA) salts are frequently used as a phase transfer catalysts in organic synthesis.[57] Due to their hydrophobic nature, they tend to accumulate at the air/water interface and act like surfactants.

The traditional way of exploring the surface activity has been surface tension measurements. Using the relation between change in the surface tension γ and surface excess of a surfactant Γ_S[56] (see Eqn. 2.6 and discussion thereof on page 20), surface composition could be deduced. However, in this picture there is no detailed structural information about the interface. Therefore, a need for experiments with surface–sensitive techniques has arisen to probe the interface on a molecular level. In case of TBA, little is known about the actual molecular structure of the interface. For example, the precise location of the iodide ion within the interfacial layer is unknown. Do the anions share the surface with cations, or are TBA and I^- segregated, forming an electric double layer?

The purpose of this publication was to shed more light into this highly relevant (from technological point of view) and interesting topic. The work was done in collaboration with an experimental laboratory that carried out photoelectron spectoscopy (PES) measurements of TBAI solutions in liquid jets. This technique is surface–sensitive, probing two or three topmost water layers. Experimental details of the work are beyond the scope of this thesis and can be found in the original publication.[8]

MD can serve as a valuable tool for interpreting experiments at the molecular level. We performed simulations of aqueous slabs containing TBA cations with iodide counter–ions. For proper description of interfacial behavior of iodide anions which is connected with

polarization,[58] polarizable force field was used. Results were analyzed by means of density profiles (showing distribution of ions across the slab), charge profiles, and orientations of TBA cations at the interface.

The experiments, where iodide photoemission signal was detected, compared TBAI and NaI aqueous solutions. Although the concentration of the latter was 80 times higher, the intensity of the photoemission signal was comparable in both cases. This directly indicates very high surface segregation of iodide in aqueous TBAI. For surface charge neutrality reasons, there has to be the same amount of TBA cations at the interface. The segregation factor (interface/bulk ratio) was estimated to be approximately 70. Additional analysis of the PES data shows that both ions share the same space at the interface and thus do not form electrical double layer. The saturation density (filling the interface with TBAI) was found by PES to be approximately 0.6×10^{14} molecules/cm^2. According to the literature, a completed surface monolayer should contain 1.0×10^{14} molecules/cm^2.[59]

Representative snapshot from the MD simulation employing 863 water molecules and 16 TBAI ion pairs is displayed in Fig. 2.2. This picture corresponds to a full coverage, which can be estimated to be approximately 0.9×10^{14} molecules/cm^2. The value compares very well with the experimental data from PES measurements mentioned above. Additional TBA cations cannot be accomodated at the interface and solvate in the bulk. Although the surface seems to have some voids, these are accomodated by very mobile iodide anions.

This is also confirmed by the snapshot and density profiles, shown in Fig. 2.2. Both cations and anions prefer the surface and their profiles overlap. This behavior of TBA is not surprising since it correlates with its surfactant activity. Presence of iodide at the interface was attributed to the effects of polarizability.[10,43,52,60] An additional effect is coming from the restriction of the total electroneutrality of the interface. Iodides thus compensate the charge of the cations.

The residual density in the bulk region corresponds to a single TBA cation that could not be accomodated at the interface and solvates in the subsurface or bulk phase. For electroneutraility reasons, it is accompanied by single iodide anion.

When Na^+, which is strongly repelled from the interface, is used instead of TBA it tends to move iodide by attractive Coulombic forces into the aqueous phase. I^- then still exhibits a surface peak, albeit smaller, accompanied by a sub–surface depletion of iodide ions.

The article also contains discussion of the charge profile across the water slab. In neat water, there is a region of positive charge at the interface (caused by dangling hydrogen atoms), followed by a negative charge region. The charge variations are extremely small (fractions of an elementary charge), but appear consistently in all simulations. In the bulk phase, the random orientation of water molecules causes the total charge to be zero. When ions are present at the interface, the situation is not changed significantly. However, in this case, the surface positive charge can be attributed to the effect of cations. Presence of ions in the bulk causes small fluctuations in the charge distribution in the interior of the slab.

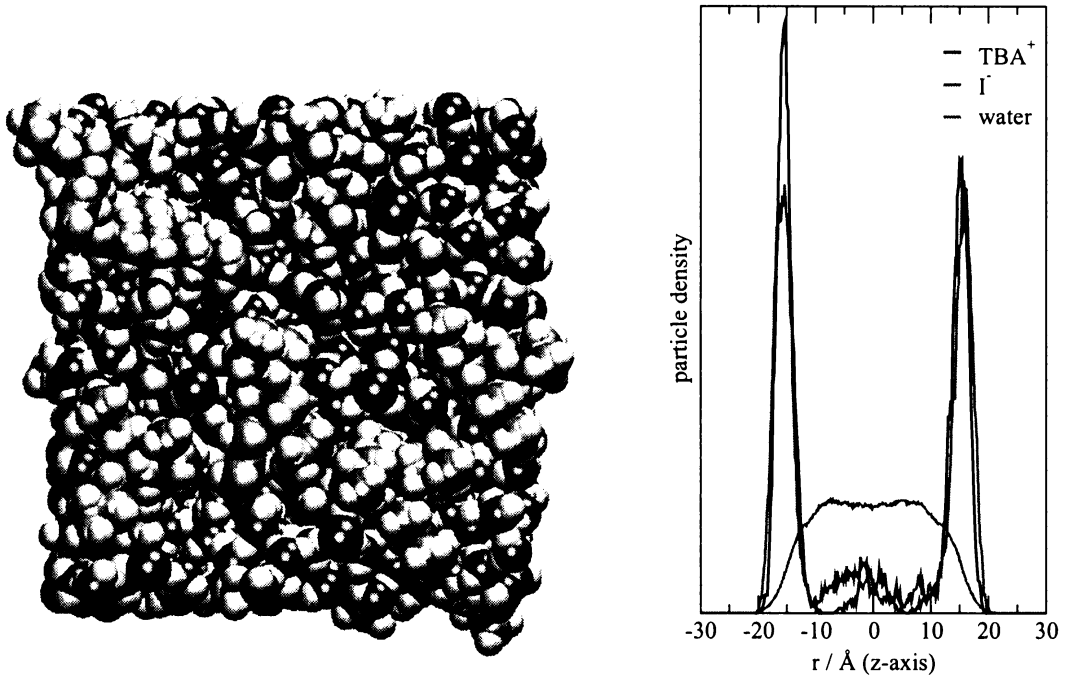

Figure 2.2: A representative snapshot of the surface of water slab and density profiles from a simulation of 16 TBAI ion pairs in a water slab. The red curve corresponds to the water signal. The iodide signal is given in violet. The density of TBA's nitrogen atoms is shown in green. Note the nearly full coverage of the surface by cations with anions occupying the remaining free space.

Total induced dipoles at the interfaces were found to point outside from the slab. Water and iodide dipoles pointing in this direction are partially compensated by the cation induced dipole oriented into the slab.

TBA is molecular ion with a flexible internal structure. We, therefore, also investigated the orientation of the butyl chains at the water interface. They have a general tendency to avoid the vapor region of the simulation cell. Mostly, they lay freely on the surface of the water slab. However, when the interface is fully covered by the ions, the chains are confined to more definite orientations. Distribution of angles between the normal to the surface and the butyl chains was found to possess 2 peaks at 90° and 150° (*i.e.*, butyl groups laying on the surface or pointing inside the water slab).

In summary, the structure of TBAI at the air/water interface was investigated using PES experiments and MD simulations. Both TBA and I^- were found to possess significant surface activity, TBA due to its hydrophobic character and I^- due to its large size and polarizability. Both ions share the same space on the surface, thus avoiding the formation of an electrical double layer. Butyl chains prefer orientations parallel to the interface and (particularly in the high salt concentrations) also pointing inside the water slab.

2.2.3 Effect of bromide on the interfacial structure of aqueous tetrabutylammonium iodide: Photoelectron spectroscopy and molecular dynamics simulations

To extend our previous study of TBA, we performed simulations that employed mixture of bromide and iodide counterions, to study the effect of different counteranions on the surface behavior of this cation.[9] Previously it was shown that iodide propensity for the interface depends also on the countercation.[8,58] Na^+, which is not surface active, tends to drag iodide towards the interior of the slab due to Coulomb attraction. On the other hand, a cationic surfactant drags iodide to the interface. The main concern of this study was the question, whether the presence of excess of bromide anions changes the surface behavior of TBAI. This problem was again studied using the combination of PES experiments and MD simulations.

As was discussed in our previous work[8], the same intensity of the iodide signal was found for NaI and TBAI solutions, however with the latter having 80× lower concentration. From these findings a segregation factor of approximately 70 was deduced for TBA.

The main effect of dissolving 0.02 m (molal) TBAI in 1 m NaBr solution was observed in the experiment as a decrease of the iodide signal by 60 % when compared to 1m NaI solution. This was rationalized by means of competition of Br^- and I^- for surface sites in the vicinity of TBA cations. The observed decrease of the iodide signal is relatively low when the difference in the concentration of respective anions is taken into account and it can be easily explained by larger propensity of iodide for the air/water interface due to its larger polarizability.

MD simulations were performed for 16 TBAI ion pairs in aqueous slab containing approximately 1 M NaBr solution (a calculation for 1 TBAI ion pair was performed as well, however is not discussed here). A representative snapshot with the respective density profile can be found in Fig. 2.3. TBA and I^- clearly prefer the interface. There is also an interfacial peak corresponding to bromide, however less intensive, consistently with its lower polarizability. It is also very slightly shifted towards the bulk phase, however, both peaks correspond to the outermost layer. Sodium cations are repelled from the interface.

When the intensity of the iodide interfacial peak is compared with the result obtained in the simulation without added NaBr, a 35% decrease can be observed. This does not compare directly to the experimental value (60%), however, the I^-:Br^- ratio in our calculations is approximately 1:1. Experimental concentrations of TBAI are not feasible in our simulations, however, it can be safely deduced that in case of ratios closer to the experiment the decrease of the peak intensity would be certainly larger.

Analysis of the charge distribution did not reveal any significant differences from the results observed for TBAI aqueous slab. Charges of TBA, I^-, and Br^- residing in the interfacial layer effectively cancel each other and remaining charge is compensated by preferrential orientations of water molecules. The water orientation also leads to the appearance of

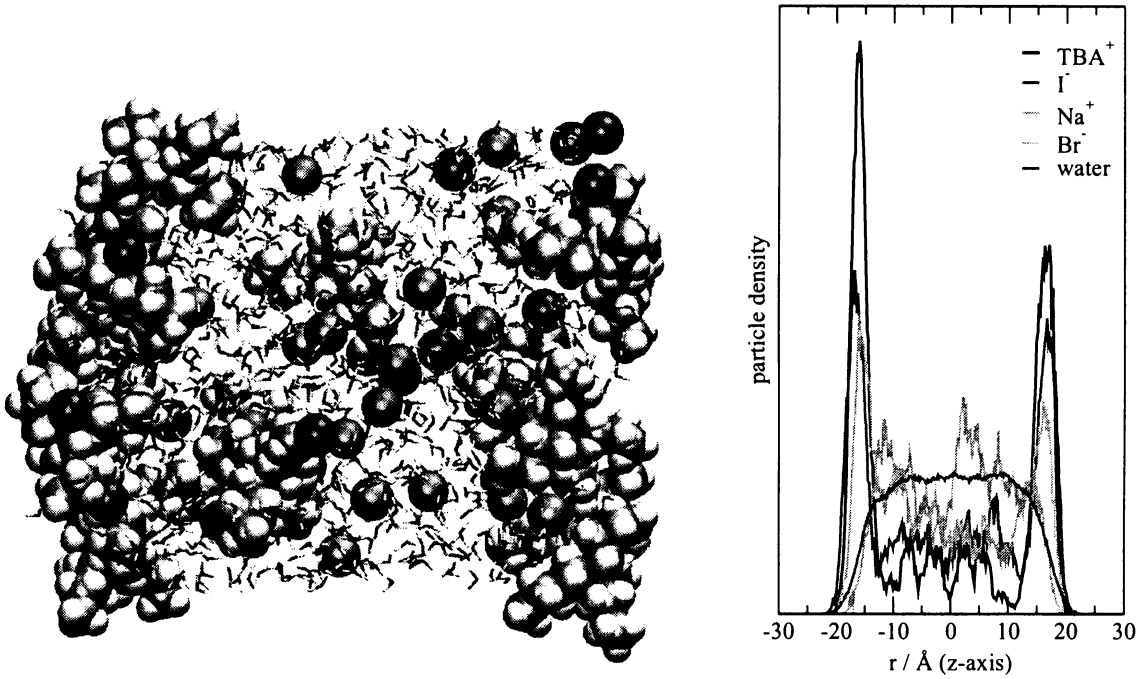

Figure 2.3: Snapshot from the simulation employing 16 TBAI pairs in aqueous 1M NaBr slab, and corresponding density profiles. Water signal is given in red. Iodides and bromides have violet and orange colors, respectively. Sodium cations are represented by green spheres.

a weak surface electric double layer, observed also in neat water simulations. Another region of positive charge can be found below this double layer. It corresponds to sodium cations attracted to the interface by Coulombic forces exhibited by the surface–bound anions.

Orientations of butyl chains are also affected by the presence of additional solute at the interface. Peaks at 90° and 150° observed for TBAI solution change to 10-40° and 170°. This difference reflects the increased particle density at the interface, forcing butyl chains to be oriented towards the gas phase, requiring thus less space.

Enrichment of Br^- and I^- at the interface is driven by their size, polarizability, and also by their tendency to neutralize the surface charge of adsorbed TBA cations. The peaks for TBA and I^- overlap, whereas Br^- (anion with smaller size and polarizability) is slightly shifted towards the bulk phase. For system with only bromide as a counter–ion, we expect similar behavior as for iodide, *i.e.*, mostly overlapping cationic and anionic density profiles, however, with a lower surface peak of Br^- when compared to I^-.

Since the propensity of bromide for the interface is lower than that of iodide, there will be more Br^- anions in the bulk phase. Due to electrostatic interactions, anions have a tendency to decrease the amount of TBA cations at the surface on a macroscopic scale. As a consequence, surface activity of TBABr is lower compared to that of TBAI.[61–63]

The most important result from this study is the finding, shown in both experiments and

simulations, that iodide is more enhanced in the interfacial layer, covered by TBA cations, compared to bromide. TBA is surface bound due to its hydrophobic character. Br^- and I^- propensities for the air/water interface can be associated with their large polarizability and size, with both properties being larger for iodide. The lower surfactant activity of TBABr when compared to TBAI can then be viewed in terms of the anionic specificity.

2.2.4 Counter–ion effects and interfacial properties of aqueous tetrabutylammonium halide solutions

Effects of different anions on the interfacial solvation of TBA cations are discussed in this article[11] in the context of our previous studies. In particular, two extremes in the halide series (large polarizable iodide and small nonpolarizable fluoride) are used as counter–ions. The effect of polarizability on the results of simulations of aqueous TBA iodide and fluoride is discussed.

For TBAI and a polarizable force field we observe a clear preference of both ions for the interface, as reported in our previous publications.[8,9] In case of 16 TBAI ion pairs in the simulation cell (we also performed for comparison simulations with a single ion pair in the water slab), that was shown to correspond to full interface saturation, strong inter–ionic Coulomb interactions lead to an enhanced accumulation of iodide at the surface, when compared to, *e.g.*, sodium iodide calculation.[34] When polarizability is not present in the force field, both ions still show preference for the interface, however iodide has a tendency to move more towards the bulk. Due to electrostatic reasons, the amount of TBA cations in the bulk is then also increased.

The difference between I^- and F^- can be easily seen after comparing the corresponding density profiles in Figure 2.4. Fluoride, as a small nonpolarizable anion is repelled from the air/water interface by image forces.[31] It is attracted towards the surface by the positive charge density caused by the TBA cations, however these forces are not strong enough to overwhelm its preference for bulk solvation. As a result, in an action–reaction process, TBA cations are shifted towards the bulk. Cationic and anionic densities are shifted with respect to each other which leads to formation of an electric double layer.

We expected to see no effect on the result of TBAF simulation when polarizability was turned off. This was true only for the calculation of a single ion pair. In case of higher concentrations, there are marked diferrences between the density profiles that we attributed mainly to the effect of water polarization.

Smaller number of particles at the interface (fluoride is bulk solvated) suggests that it should be possible to accomodate more cations than in the case of, *e.g.*, TBAI. Analysis confirms that there indeed is more free space available, however, high positive charge density results rather in a higher probability of transfer of cations into the bulk phase.

Charge distribution across the water slab (see Fig. 2.5) is consistent with our previous finding. Directly at the interface there is a region of positive charge attributable mainly

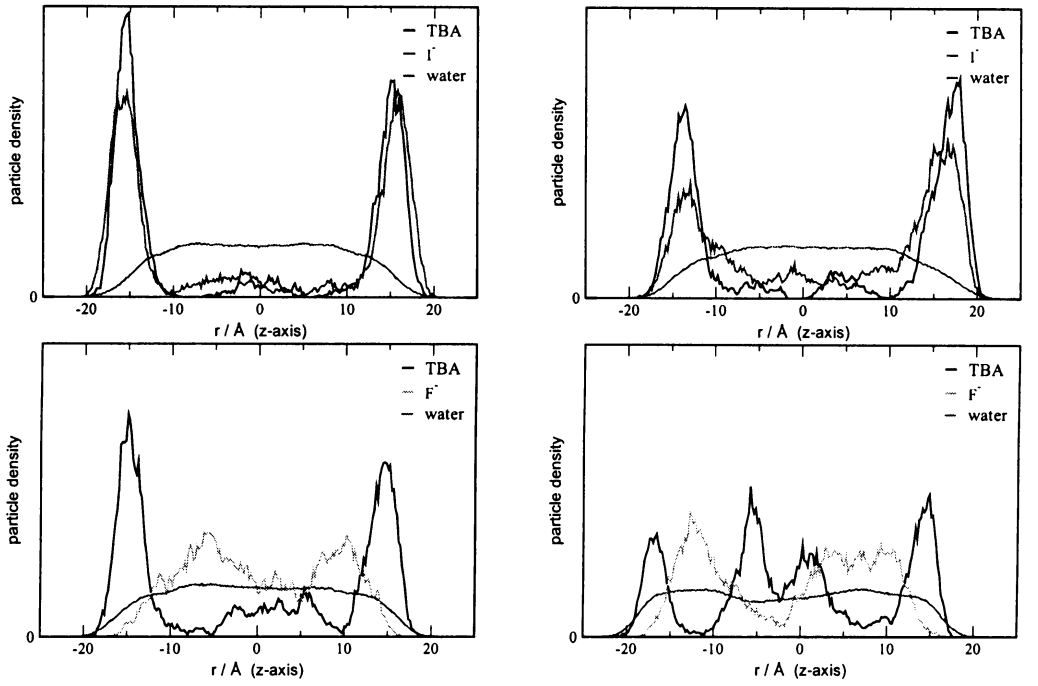

Figure 2.4: Density profiles from TBAI (top) and TBAF (bottom) simulations. Results for both polarizable (left) and nonpolarizable (right) force fields are shown.

to the dangling hydrogen atoms. As was noted before, the charge fluctuations are very small, however, consistently present in all our simulations. In TBAI, the charges of the ions present on the surface effectively cancel each other. Surprisingly, even for TBAF, there is only small net charge, probably due to preferrential orientation of water molecules. The region of negative charge in the subsurface is more influenced by the ion distribution, affected by the different propensity of anions for the air/water interface and by the type of force field used. The total charge density in the bulk oscillates around zero.

Size and orientation of induced dipoles are strongly influenced by the distribution of ions. In the bulk phase, random orientation of water molecules results in an almost zero net electric field and negligible induced dipoles. At the interface, the biggest difference between salts can be observed for simulations corresponding to a full surface coverage. For TBAI, the total dipole points out of the slab.[8] On the other hand, the total induced dipole has the opposite orientation (towards the bulk) when fluoride is used as a counterion.

Orientation of butyl chains with respect to the normal to the surface is almost the same for polarizable and nonpolarizable force fields and does not show any profound counterion specificity. At surface saturation concentration (16 TBA cations), the orientations of butyl chains are bimodal (90° and 150°) due to sterical confinement of a large amount of molecules adsorbed at the interface.

To conclude, we performed MD simulations of aqueous slabs of TBAI and TBAF. Propensities of individual ions for the air/water interface were investigated. Effects of counter–ions

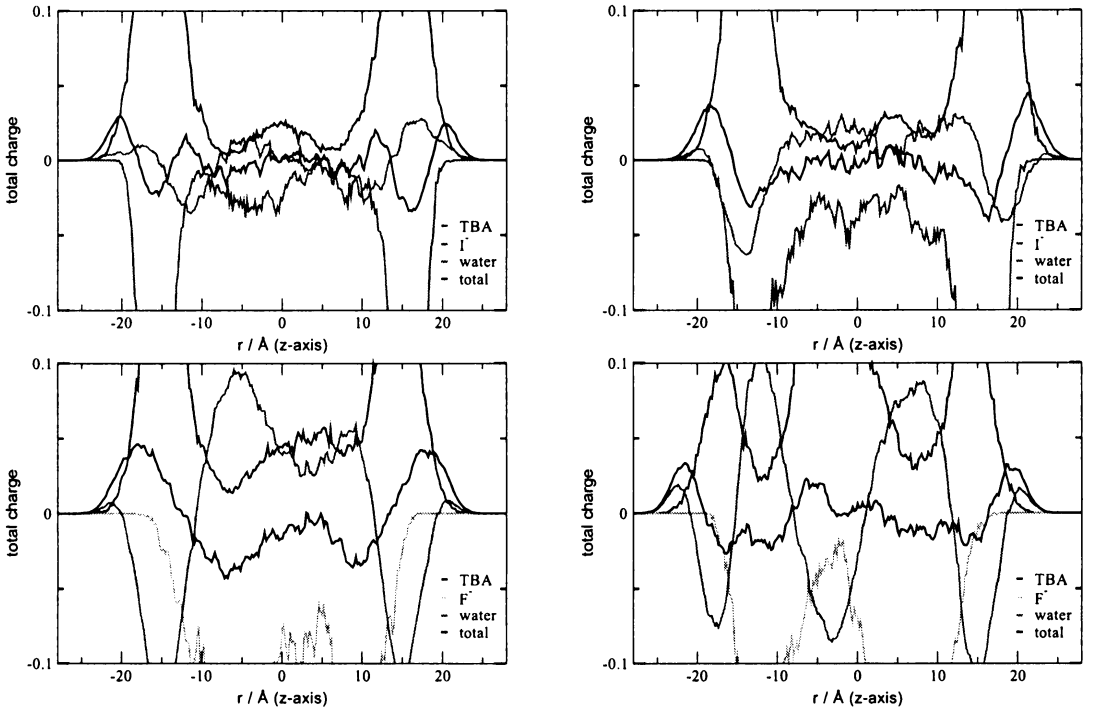

Figure 2.5: Charge profiles from TBAI (top) and TBAF (bottom) simulations. Results for both polarizable (left) and nonpolarizable (right) force fields are shown.

and the role of polarization interaction were taken into account. Iodide, driven to the interface by its large size and polarizability markedly differs from bulk–solvated nonpolarizable fluoride. TBA cations are expelled from the bulk due to hydrophobic forces. At high concentrations the ion–ion interactions become significant and strongly influence the density profiles across the water slab.

2.2.5 Selected biologically relevant ions at the air/water interface: A comparative molecular dynamics study

In our MD study of the effect of ions on the enzymatic activity of horseradish peroxidase[17] (see section 4.2.1) we studied several ions, namely sodium and choline (2-hydroxyethyl–trimethylammonium) cations, and chloride and sulfate anions. The behavior of these ions at the air/water interface, as well as solvation properties of four simple tetraalkylammonium (TAA) cations with sulfate and chloride as counter–ions are reported in this article.

The hydration properties of TAAs can be tuned by the choice of the length of the alkyl chains. TAA cations (*e.g.*, TBA) are often used as phase transfer catalysts in technology and industry.[57] Due to their properties, they are capable of transporting small ions across biological membranes and block cellular ion channels, which explains their potential toxicity.[64,65] The solubility of TAAs in water decreases with increasing length (hydrophobicity)

of the alkyl chains. Larger cations exhibit surfactant properties.

In our previous studies of TBA[8,9,11] we quantified its surface activity and studied varying interfacial behavior of different halide counter–ions. Bromide and particularly iodide strongly co–adsorb at the interface. On the other hand, fluoride resides in the subsurface and bulk of the solution, affecting also TBA distribution.

Choline can be regarded as another cation with imortant biological functions. It is a basic constituent of phospholipid membranes and serves as a precursor for acetylcholine and betaine.[66] It can also affect enzymatic activity. A recent study of horseradish peroxidase revealed that choline chloride can counteract the sodium sulfate induced superactivity in this enzyme.[67] Our simulations showed that this effect could be ascribed to the affinity of choline to hydrophobic residues of the protein in the vicinity of the active center.[17]

We performed MD simulations in the slab geometry, empolying a polarizable force field, of TAAs (with one to four carbons in each of the alkyl chains) and of choline with chloride or sulfate counter–ions.

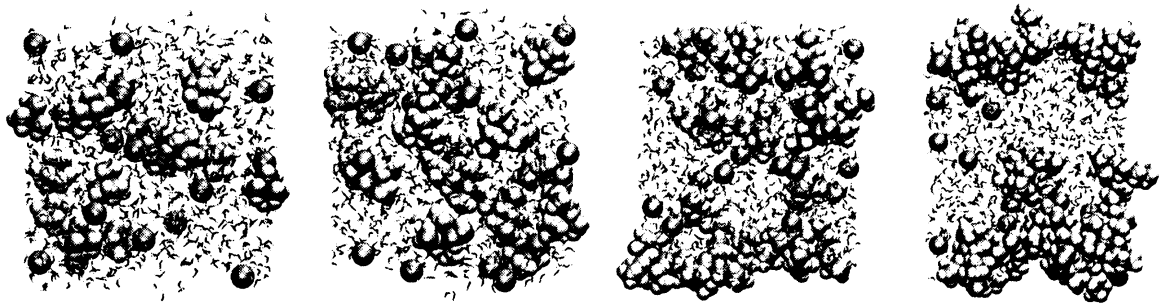

Figure 2.6: Snapshots from TAA simulations with chloride (orange spheres) as a counterion. Figures correspond to TMA, TEA, TPA, and TBA (left to right). Air/water interfaces are located in the top and bottom parts of the figures.

Figure 2.6 shows representative snapshots from the TAA chloride simulation, the density profiles can be found in the original publication.. As can be expected, the propensity of individual cations increases with increasing length of the alkyl chains (hydrophobicity). Tetramethylammonium (TMA) is repelled from the interface, similarly to alkali cations. Density profile of tetraethylammonium (TEA) closely follows that of water, indicating its surface neutral character. Both tetrapropylammonium (TPA) and TBA behave as typical ionic surfactants, consistently with our previous studies.[8,9,11]

The investigated anions behave very differently from each other. Chloride exhibits a weak propensity for the interface due to its relatively large polarizability (the propensity is, however, much weaker than that of iodide or bromide). Sulfate is strongly repelled from the interface by electrostatic forces. However, the effect of counterions on the surface propensities of TAA cations is weak. Weakly surface attracted chloride cannot pull any significant amount of TMA towards the interface. On the other hand, bulk solvated sulfates are not able to pull surface active TPA and TBA into the bulk phase.

Figure 2.7: Snapshots from choline simulations with chloride (left), sulfate (middle) and chloride/sulfate mixture (right) as counterions. Air/water interfaces are located in the top and bottom parts of the figures. Color coding: Cl^- - orange, Na^+ - green.

In none of the simulations we performed for choline (choline chloride, choline sulfate, choline chloride and sodium sulfate mixture, see Fig. 2.7) any preference of the cation for the air/water interface was observed. This is in striking contrast with its affinity to protein surface.[17] It is rather repelled from the air/water interface despite its relatively large size. This can be clearly seen particularly in the choline sulfate solution. With chloride as a counterion, choline is moved closer to the interface by the negative charge present there due to anions at or near the surface.

The situation is more complicated and more interesting in the mixture of choline chloride and sodium sulfate. Chloride shows a weak propensity for the air/water interface, similarly to pure alkali chloride solutions.[34,52] Sodium and sulfate ions are solvated in the bulk and their charges compensate each other. Choline exhibits an intermediate behavior with appreciable subsurface peak, compensating the chloride charge.

In summary, we performed MD simulations of selected biologically relevant ions in the slab geometry, employing a polarizable force field. For small TAA cations, we have shown the shift from bulk to surface solvation upon increasing the length of the aliphatic chain. TMA solvates in the aqueous bulk, TEA exhibits intermediate behavior, while TPA and TBA clearly possess surfactant properties. The effect of counterions on the surface propensity of the cations is very weak. Choline was shown to be repelled from the air/water interface. However, with chloride as a counterion, choline shows a weak subsurface propensity. The behavior of choline, sulfate, sodium, and chloride ions was found to have no correlation with their properties at the solution/protein interface.[17]

2.2.6 Aqueous ionic and complementary zwitterionic soluble surfactants: Molecular dynamics simulations and sum frequency generation spectroscopy of the surfaces

Amphiphilic species (consisting of both hydrophilic and hydrophobic parts) constitute a group of technologically and biologically very important chemical substances. Owing

to their structure, they tend to form two–dimensionals films at the air/water interface. This behavior can be described in thermodynamic terms of surface tension and surface excess (Eqn. 2.3), and by the Gibbs adsorption isotherm (Eqn. 2.4).

MD simulations and surface sensitive experimental techniques can go beyond the integral surface excess description and provide information with atomic resolution about the distribution and orientation of surfactant molecules in the interfacial layer.

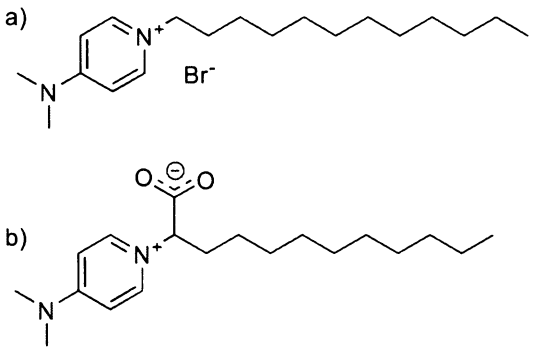

Figure 2.8: Chemical structures of (a) 1-dodecyl-4-(dimethylamino)pyridinium (DMP) bromide, and (b) 2-[4-(dimethylamino)pyridinio]dodecanoate (DPN).

We studied soluble ionic surfactant, 1-dodecyl-4-(dimethylamino)pyridinium (DMP) bromide, and its related zwitterion, 2-[4-(dimethylamino)pyridinio]dodecanoate (DPN), in water and in aqueous solutions of KF and KBr. Structures of both molecules are displayed in Fig. 2.8.

Dimethylamino and pyridinium groups forming the headgroup create a so–called push–pull system, resulting in high hyperpolarizability and, consequently, in nonlinear optical activity. Therefore, both substances can be studied using surface–selective nonlinear optical methods such as the SHG spectroscopy. Such experiments can characterize the structure of the interface with respect to surfactant distribution. Previously, the strong change in adsorption behavior of DPM bromide upon addition of potassium salts was found.[68]

In the present study, SFG spectroscopy experiments for DMP bromide with and without added salts have been carried out to observe changes in the aliphatic chain conformations and water structure at the interface. MD simulations have been performed to help in the interpretation of the experimental data.

Results of the calculations are discussed briefly. Both the cationic DMP and the bromide anions prefer the surface regions. The surface segregation of the cations is very strong due to their hydrophobic tails. Bromide anions are driven towards the interface due to their polarizability and (at higher concentrations) due to surface neutralization effects. However, the preference of anions for the interface is much weaker than that of cations, resulting in more diffuse anion distribution.

Density profiles of systems containing DMP confirm the preferential orientation of the amphiphiles, with hydrophilic part anchored in the water phase and aliphatic chains pointing into the air. Upon addition of more cations corresponding to a full surface coverage the formation of a sublayer is observed. In lower concentrations, aliphatic chains are free to fold and unfold at the interface. At higher concentrations the mobility of individual chains is significantly decreased. Upon addition of KF and KBr into the simulation cell an interesting behavior was observed. Potassium cations are repelled from the interface due to repulsion from cations present at the interface and also due to image charge repulsion.[31] Fluoride generally prefers bulk solvation. However the high charge density at the interface results in weak subsurface propensity of F^-. Bromide that itself shows some surface propensity is (at appreciable DMP concentrations) strongly enhanced at the interface.

Surface behavior of zwitterionic DPN is very similar to that of cationic DMP. For higher concentrations, formation of a surfactant sublayer is observed. DPN molecules in the topmost layer prefer bent conformations with a sharp angle between the aliphatic chain and the hydrophilic moiety. Carboxylate is oriented towards the water phase and repelled from the alkyl group. At higher concentrations the subsurface species are more straightened (due to sterical reasons). In simulations with KF, both potassium and fluoride reside in the bulk phase. DPN therefore behaves differently from DMP, where attraction of anions to the surface or subsurface due to surface neutralization can be observed. For simulations with KBr, bromide nevertheless exhibits a surface peak due to its inherent propensity for the air/water interface.

The analysis of headgroup orientation shows its appreciable dependency on concentration. The headgroup orientation peaks at 60° for small concentrations and it shifts to 30° for higher ones. For small concentrations of DPN the headgroup preferred orientational angle is 120° an the preference changes to smaller values with increasing concentration. The differences between DMP and DPN are primarily due to the streric interaction of the carboxylic group. The calculated angles are in good agreement with results of SHG measurements. However, detailed discussion of the experimental results is beyond the scope of this thesis. Relevant information can be found in the original paper.

In summary, we performed MD simulations of ionic DMP bromide and zwitterionic DPN. Both molecules strongly adsorb at the interface. At higher surface coverages a buildup of a sublayer was observed. Bromide anions mostly coadsorb at the interface due to their polarizability and presence of DMP cations. Addition of KF has little effect on surface behavior of both DMP and DPN. KBr affects the interface much more strongly due to sizable affinity of bromide to the surface. These findings are consistent with the results of SFG and SHG spectroscopy experiments.

2.2.7 Interior and interfacial aqueous solvation of benzene dicarboxylate dianions and their methylated analogues: A combined molecular dynamics and photoelectron spectroscopy study

Dicarboxylic acids are recognized as a class of global atmospheric pollutants and they form a major component of urban aerosol samples.[69,70] They also play an important role as cloud condensation nuclei[71,72] and are responsible for the formation of many secondary organic aerosols.[73] Understanding of (micro)solvation of dicarboxylic acids and their behavior at the air/water interface is, therefore, very important for atmospheric chemistry.

We studied using MD simulations aqueous solvation of *o*-, *m*-, and *p*-benzene dicarboxylate dianions (BCD^{2-}) as well as tetramethylated *o*-BCD^{2-}, with the focus on the competition between electrostatic and hydrophobic interactions determining the solvation properties. The work was done in cooperation with an experimental laboratory which carried out photoelectron spectroscopy measurements on benzene dicarboxylate dianions in water clusters.

Experimental findings will now be summarized shortly. PES of *o*- and *p*-BCD^{2-} with up to 25 water molecules indicate interior solvation of the dianions. For the para–isomer, alternate solvation of the two separated charged groups was observed. The same effect was recently found in the analogous study of aliphatic dicarboxylates.[74,75] In the case of ortho–isomer, such behavior was not observed due to the fact that both carboxylate groups are in a close proximity and can be solvated simultaneously by a single water molecule.

Solvation properties of BCD^{2-} are determined by the interplay between the hydrophobicity of the benzene ring and hydrophilicity of the carboxylate groups. It is not apparent which of these effects prevails, so MD was used to shed more light into this interesting problem.

In all cases (*o*-, *m*-, and *p*- isomers) employing both polarizable and nonpolarizable force fields, hydrophilicity of the anionic groups is the dominant driving force and all three dianions solvate in the bulk phase, leaving an ion–free surface layer. However, with inclusion of polarization (favoring asymetrically solvated species[10]) the ion–free layer becomes thinner. Also, the isomers with carboxylate groups in closer proximity (*o*- and to a lesser extent *m*-) show tendency to orient in the subsurface.

Due to different solvation properties of the two parts of BCD^{2-}s the hydration shell is asymmetric. This can be clearly seen in Figure 2.9 that shows closest 25 water molecules around the *p*-BCD^{2-} molecule. Water structure around the carboxylates is dense and compact. On the other hand, the water solvation layer of the benzene ring is very diluted and shows many voids.

The balance between hydrophobic and hydrophilic forces can be easily shifted via methylation of the benzene ring. Tetramethylated *o*-BCD^{2-} clearly prefers interfacial solvation, regardless on the force field used (polarizable or nonpolarizable). This is consistent with our previous findings that polarization effects are rather unimportant for the solvation

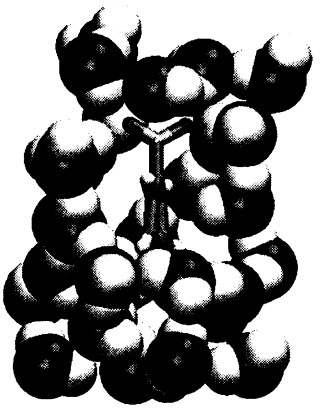

Figure 2.9: First solvation shell (25 water molecules) of p-BCD^{2-}. Note the dense water structure around both carboxylates and clearly visible voids around the benzene ring.

properties of hydrophobic surfactants (*e.g.*, TBA).[8,9,11] Tetramethylated benzene dicarboxylate is strongly oriented at the interface. The two carboxylate groups are anchored in the interfacial water layer with the benzene ring pointing into the gas phase being, however, strongly tilted or laying on the surface.

Using computer simulations we studied solvation properties of benzene dicarboxylate dianions in aqueous slabs. All three isomers of BCD^{2-}s prefer bulk solvation, regardless of the use of polarizable or nonpolarizable force field. Tetramethylation changes this behavior into the preference for interfacial solvation. For tetramethylated o-benzene dicarboxylate strong orientational preference at the interface is found. Carboxylate groups are anchored in the slab, with hydrophobic aromatic ring laying on the surface.

2.3 Future perspectives

An obvious disadvantage of the classical MD approach is the necessity to employ an empirical interaction potential. Ideally, an ab-initio quantum mechanical approach which works only with fundamental physical constants should be used. This is, however, practically impossible due to extreme demands on the computer power and storage. With further advancement in computer science, first calculations of this kind are being published in the literature. Recently, Mundy and coworkers reported results of pioneering first principles simulations of a slab of liquid water and discussed the applicability of this approach to the simulations of extended aqueous systems.[76–78]

As discussed in the previous text, MD simulations predict the enhancement of some of the polarizable anions at the air/water interface. This is in disagreement with the classical theory of surfaces of electrolytes presented by Onsager and Samaras.[30,31] However, results of the surface-sensitive techniques such as SFG, VSFG, and PES confirm in many cases

the predictions of the conceptually simple MD techniques.[8,35,36]

Nevertheless, there are still many problems open. The experiments involving aqueous interfaces are inherently difficult. Very often, their interpretation is not particularly straightforward and conflicts between the experimental and theoretical results can arise. Also, the reliability of the simualation depends on the quality of the interaction potential used. It is always necessary to make a tradeoff between the efficiency of the model and its accuracy (more accurate and more sophisticated models tend to be computationally more demanding). A related problem of the most frequently used empirical potentials is their incapability to describe bond dissociation. Compared to the classical MD software packages, the software for ab–initio simulations also generally requires much more user intervention and knowledge about the details and intricacies of the method used.

Methods of ab-initio molecular dynamics do not rely on an empirical potential. The potential in which the atoms move and forces are evaluated from first principles using only fundamental physical constants. However, even in this case several approximations are applied.

The most frequently used method for the evaluation of the ab–initio MD potential is the plane–wave density functional theory (DFT). Plane waves are a natural choice for the description of systems with periodicity. Their simple mathematic form allows for very fast evaluation of electronic integrals in the Schrödinger equation. On the other hand, very large number of plane waves needs to be used in the linear expansion of one–electron functions. Energy cutoff is usually employed so only waves up to certain energy are used to save computer time. Contrarily, the description of core electrons requires waves with very high energy. Since most of the properties depend dominantly on valence electrons the so–called pseudopotential approximation is used. Only valence electrons are treated explicitly, while nuclei and core electrons are represented by the pseudopotential. The pseudopotential as well as the DFT functional have to be carefully chosen depending on the studied problem. Another shortcoming is that the most frequently used functionals do not provide correct description of dispersion forces.

There exist two basic strategies for ab–initio MD. In Born–Oppenheimer MD the nuclear degrees of freedom are propagated using ionic forces that are calclated at each iteration by approximately solving the electronic problem by conventional matrix diagonalization methods. On the other hand, the Car–Parrinello method introduces the electronic degrees of freedom as fictitious dynamical variables, which leads to a system of coupled equations of motion for both ions and electrons. In this way an explicit electronic minimization at each step is not needed. While the former method is much more computationally demanding, the latter requires the introduction of an additional parameter, and also use of much shorter timestep to keep the calculation numerically stable.

As a consequence of the used methodology, these calculations are extremely demanding with respect to computer power and memory capacity. However, advance in computer technology and also in theoretical methods make these calculations a clear target for future work.

Chapter 3

Ions at the ice/water interface – A simulation study of brine rejection

3.1 Introduction

Water is probably the most important and the most intensely studied substance on Earth. It is of vital importance in many aspects of our existence, ranging from cloud microphysics to its key role as a solvent in many chemical reactions. The familiar process of water freezing is encountered in many natural and technologically relevant processes. We will now discuss the applicability of methods of computational chemistry for the theoretical study of brine rejection from freezing salt solutions.

Sodium chloride and other common inorganic salts are very poorly soluble in ice, with solubilities in the micromolar range at best.[79] Liquid water, however, is capable of dissolving molar amounts of these salts. This property is clearly demonstrated by the fact that the salinity of the sea ice is much smaller than that of seawater. When an aqueous NaCl solution freezes above its eutectic temperature (-21.1 °C)[80] it solidifies as almost pure ice. The salt is rejected into the surrounding unfrozen solution. Salt concentration and temperature gradients due to latent heat release are established across the freezing front as freezing proceeds. This results in the formation of macroscopic instabilities and the initially planar freezing front becomes corrugated.[81–83]

When freezing occurs on the surface of the ocean, the rejected salt increases the density of the underlying water masses. This leads to massive circulations in the ocean influencing the global climate.[3] Brine rejection is also proposed to play an important role in the thundercloud electrification.[84] Supercooled cloud water droplets containing salt particles originating from the soluble cloud condensation nuclei can freeze upon impact forming the so-called graupels. Dissolved salt is then rejected from the freezing water and concentrates on the surface of the graupel. The electrification then occurs via collisions between neat ice crystals and salt-covered graupels.

Brine rejection is thus an extremely interesting and also important process with wide natural, atmospheric, and technological consequences (desalination being a prominent example of the latter). It has, therefore, been subject to experimental[85] as well as theoretical research.[86]

A key point in the simulations is the choice of the interaction potential. There exist many different water models optimized for different purposes.[87] Each model shows better or worse agreement for particular water properties. These models are mostly fitted to describe liquid water. Therefore, their use for simulations of ice can be tricky. Namely, one of the properties that is often described incorrectly is the melting temperature. A comprehensive comparison of the most common water models with respect to the melting temperature of water has been published recently.[88] Values in a wide range of 190 to 270 K were obtained. It is, therefore, always necessary to choose between the computer efficiency of the model and the quality of the description of water properties, although a more complicated model does not always mean better description.

We applied the MD technique to simulation of brine rejection from freezing salt solutions employing the rigid 3-site simple point charge (SPC/E) water model.[89,90] Our goal was to obtain the microscopic picture of this very important natural process.

3.2 Summary of results

Our calculations[15] can be viewed as an extension of the work of Bryk and Haymet.[91] They studied the behavior of Na^+ and Cl^- ions at the static ice/water interface on the nanosecond timescale. We were interested in the crystallization process itself and in the expulsion of the ions into the remaining liquid. This required using long simulation times (hundreds of nanoseconds). For the purpose of our research, we used the SPC/E water potential[89] together with potential parameters for sodium and chloride from Ref.[92].

We have investigated freezing of water and salt solutions in contact with a layer of cubic ice Ic, which is a metastable form of the most common hexagonal ice Ih. These two possess very similar properties (structure, density, heat capacity, etc.). Also, the cubic (rather than hexagonal) ice is involved in several important processes. Water in nanopores was shown to freeze in this crystal modification.[93] A key role of ice Ic in cloud formation was proposed.[94–96] Moreover, cubic ice was found to be predominantly formed during freezing of small water droplets (radius up to 15 μm) or thin water films (thickness up to 10 μm).[97]

Firstly, we performed series of freezing/melting simulations of an ice layer in contact with neat water for a range of temperatures around the melting point of the SPC/E water model (which was assigned relative value of 0°). These calculations were necessary for establishing a robust simulation protocol for ice/water simulations with the employed potential model. Supercooling to -15 ° was found to provide fastest freezing rates and was used in the simulations involving salt solutions.

Neat water calculations also revealed the timescales of the (simulated) freezing process. Previous simulation studies of the coexistence of ice with liquid were done on the timescale of hundreds of picoseconds up to 2 ns.[98–100] Our work indicates that the time needed to observe significant changes in the interface are in order of hundreds of nanoseconds, *i.e.*, 2 – 3 orders of magnitude longer than in previous simulations. Even melting close to the melting point takes several tens of nanoseconds in the MD run. The situation is now slowly changing thanks to the appearance of new water models with the melting temperature close to 0°C,[101–103] however the timescales are still of the order of nanoseconds to tens of nanoseconds.

Simulations of brine rejection from freezing salt solution were run at the temperature of -15 °, consistently with the optimal neat water simulation conditions. The time needed to freeze the simulation cell significantly increased with the increasing concentration. The kinetic anti–freeze effect of the added salt was thus demonstrated at the molecular level.

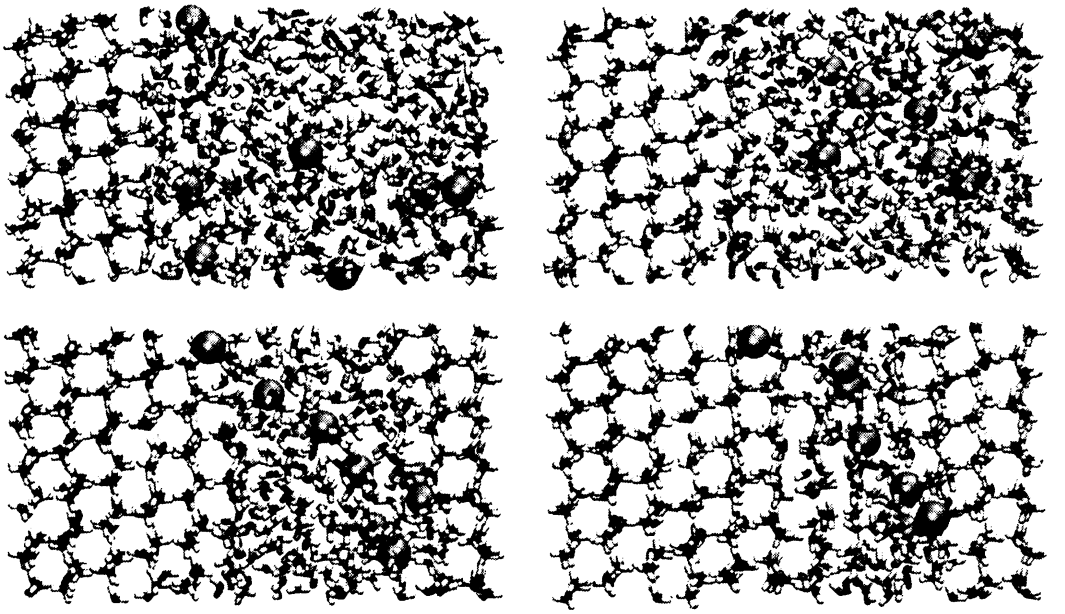

Figure 3.1: Snapshots from the freezing simulation of 0.3M salt solution taken at 1, 200, 400, and 600 ns. Na^+ and Cl^- are given as green and orange spheres, respectively.

The progress of the simulation is shown in Figure 3.1. In the beginning, there is a patch of ice in contact with salt solution. Gradually, as more and more water is incorporated in the ice lattice, the ions concentrate in the remaining part of the solution, finally forming a thin layer of unfrozen brine. This region has a glassy character and shows a slow tendency of incorporation of additional water molecules into the ice lattice. However, a complete equilibrium between the brine and ice regions is not established on the timescale of the simulation.

As seen on the snapshots, ions can be sometimes trapped in the ice lattice. We observed

only trapping of chloride (sodium was never trapped). This correlates nicely with the results of recent calculations of NaCl placed at the ice surface, which showed some degree of charge separation.[91] However, to obtain statistically significant data, it would be necessary to perform many more extremely time demanding calculations with prohibitively large simulation cells.

The results also provide information about the dynamical mechanism of brine rejection. Based on our calculations we propose the following scheme. The progression of the freezing front and the expulsion of the ions are highly correlated. Firstly, there is a fluctuation (reduction) of the salt density close to the interface followed by the buildup of a new ice layer. For a proper quantification of this mechanism, many more simulations would need to be performed, however the atomic picture is emerging already from the present data.

In summary, the freezing of water and salt solutions in contact with an ice layer was investigated using the MD simulations. A robust simulation protocol for reproducible freezing of SPC/E water was established. We observed brine rejection in freezing solutions with varying salt content. At the molecular level, NaCl was shown to act as an antifreeze agent. A molecular mechanism correlating salt density fluctuations with the progression of the freezing front was proposed.

3.3 Further studies

3.3.1 Homogeneous freezing of water starts in the subsurface

We used a recently proposed 6-center water potential[101] (abbreviated NE6) for simulation of water freezing 'from scratch' performed in a slab geometry. The ultimate goal was to provide a computational view on the surface-induced homogeneous ice nucleation. This project is beyond the scope of this thesis, so it will be only briefly discussed here. The results will be used in the follow–up study of homogeneous freezing of salt solutions in geometries involving the air/water interfaces.

In most cases, water in nature freezes heterogeneously, i.e., in contact with crystallization nuclei such as small pieces of ice or minerals. When such contact is avoided, water can be supercooled to very low temperatures (below -30°C) before homogeneous freezing takes place.[104] Droplets of supercooled water are known to be formed in the stratosphere and upper troposphere.[105,106] Homogeneous nucleation is the controlling mechanism for the formation of cirrus and polar stratospheric clouds, affecting directly the radiative balance of the Earth.

There exists an ongoing scientific debate whether homogeneous nucleation starts at the surface or rather in the bulk of the water droplet. The experimental evidence in this case is ambiguous. It has been concluded recently that, based on existing thermodynamic nucleation models, as well as laboratory and atmospheric data, ice nucleation at the surface can be neither confirmed nor disregarded.[107] On one hand, recent laboratory experiments

indicate that homogeneous ice freezing is a volume proportional process with surface nucleation being potentially important for small droplets with radii below 20 nm.[108] On the other hand, higher freezing temperatures and faster freezing rates were observed for droplets with an ice forming nucleus placed close to the surface compared to a bulk location.[109] It has been suggested recently that molecular simulations could provide further information concerning the surface initiated homogeneous nucleation.[110]

Thanks to advancement of computer technology molecular simulations of processes related to water freezing are becoming feasible. The greatest advantage of the calculations is that they can provide an insight into the structure and dynamics of the system at an atomic level, with resolution often inaccessible to experimental techniques.

Crystallization usually involves very long time scales (at least when compared to the time scales of routine calculations) and complicated potential energy landscapes. Computer simulations of this process are, therefore, considered to be difficult in general. In a series of papers, Haymet and coworkers investigated the structure and dynamics of the ice/water interface.[98,99,111] In their approach, the prebuilt patches of water and ice were put together to create the interface. The necessity to simulate the highly improbable creation of the crystallization nucleus was thus avoided. A similar setup was used by other groups to assess various properties of the ice/water interface.[102,103,112–114] These simulations can be easily extended to systems containing solutes, namely simple salts,[91,115] as in our work summarized in Section 3.2.[15]

Water freezing was observed in simulations of systems subjected to an electric field,[86] in confined water,[116] and in (non-dynamic) Monte Carlo calculations.[117] However, there have been to the best of our knowledge only two successful MD simulations of water freezing from scratch, *i.e.*, without any bias introduced by initial conditions (an existing crystallization nucleus or external electric potential).[118,119]

We performed calculations that could indicate whether homogeneous water freezing starts in the bulk phase or at the interface. We employed slab periodic boundary conditions (see Section 1.4.1), that are particularly suited for this purpose. We showed that the nucleation process is most likely to occur in the subsurface of the water slab.[120] On one hand the bulk phase does not have enough mobility to allow fast reorientation of water molecules and to efficiently accomodate the volume change upon freezing. On the other hand, waters directly at the interface are too mobile and undercoordinated. Therefore, the subsurface is the preferred location.

3.3.2 Homogeneous nucleation of aqueous solutions

As was discussed in Section 3.3.1, we established a robust protocol for simulating the homogeneous nucleation of water.[120] In a follow–up study, we intend to perform MD calculations that should provide information about how different solutes (NaCl, aliphatic alcohols with short and long chains, etc.) affect the nucleation process. These simulations can provide a highly relevant information in the field of atmospheric chemistry.

Chapter 4

Ions at the protein/water interface – biological consequences

4.1 Introduction

Studies of ion effects in biological systems have been carried out for more than a century. In 1880s, Hofmeister with coworkers published a series of papers showing how salts could be classified according to their ability to salt out proteins.[55] Similar trends were found for other effects in biological systems, but also for various interfacial properties such as surface tension.[121]

A question now arises, whether the Hofmeister series is strictly related to interfaces. Also, can a protein be regarded as an entity with well defined surface? The majority of the ion–protein effects seems to be highly specific. For example, only some aminoacid types were found to be involved in the binding of sulfate and phosphate anions.[122] The balance between different ionic effects (salting in, salting out, protein folding, etc.) is indeed very subtle,[123–126] depending also on other conditions (nature of a protein, pH, or concentration).

Very often simple models are used to describe these complex and subtle effects.[122,127] Recently it was suggested, that a protein can be regarded as simplified object having a certain surface and that its interactions with ions can be described by electrostatic and dispersion forces. The molecular details of the surface are averaged out by protein motion. Ions, therefore, experience a nearly homogeneous surface.[128] In this approach, however, many important details, *e.g.*, granularity of solvent, are neglected. Hofmeister series for ions near proteins and air/water interfaces were correctly predicted using this model. However, a simultaneous description of bulk activity coefficients and surface tension failed.[129]

In our work, we attempt to overcome the shortcomings of this model by employing MD simulations for the study of properties of ions in the vicinity of proteins. Using the results providing atomic level details we are tracking down the importance of individual ion – protein interaction. In this picture, a protein can be rather viewed as a collection of

functional groups than a single homogeneous object. Also, the possible effects arising from the the interactions with solvent can be tracked down, contrary to solvent averaged models.

4.2 Summary of results

Our studies of the ion–protein interactions concerned two separate projects. In the first one, discussed in Section 4.2.1, we examined the behavior of two proteins in choline chloride and sodium sulfate solutions.[16] In the second study,[17] we quantified the reasons behind the fact that sodium shows higher affinity to the protein surfaces than potassium. The results are summarized in Section 4.2.2.

4.2.1 Specific ion effects at protein surfaces: A molecular dynamics study of bovine pancreatic trypsin inhibitor and horseradish peroxidase in selected salt solutions

In their recent articles,[67,130] Kunz and coworkers experimentally examined the effect of various salts (sodium sulfate, tetramethylammonium sulfate TMAS, tetramethylammonium bromide TMAB, and choline chloride) on the enzymatic activity of horseradish peroxidase (HRP). From the known dependencies of the ion activity on pH, and of pH on concentrations of different salts, they proposed the relation between the enzymatic activity and salt concentration.

For sodium sulfate, the change in the enzymatic activity could be completely explained by the pH change of the solution upon adding the salt. However, in other cases, the change in activity could not be ascribed solely to the effect of pH. In fact, quaternary ammonium salts showed antagonistic behavior with respect to sulfate. The superactivity induced by SO_4^{2-} anions could be balanced by a stoichiometric amounts of, *e.g.*, choline cations.

We performed MD simulations of two proteins (HRP and bovine pancreatic trypsin inhibitor BPTI) in several aqueous salt solutions – sodium sulfate, sodium chloride, choline sulfate, choline chloride, and their mixture. HRP was chosen for continuity with the experiments. BPTI served as a model system. Due to its small size, it was a very computationally efficient test case. The analysis of the trajectories provided the distribution of individual ionic species in the vicinity of the protein 'surface' and also gave information about ion specific adsorption to different amino acid residues. To see the difference between ion preference for the air/water and protein/water interfaces we also carried out analogous simulations of aqueous solutions of the same ions in the slab geometry.[12] The results are discussed in Section 2.2.5 of this thesis.

The term *protein surface* will be used frequently in the following text. By this we mean all protein atoms accessible to the surrounding aqueous solution. Additional term, *ion binding*

Figure 4.1: Representative snapshots of BPTI and HRP in the mixed sodium sulfate and choline chloride solution. Water molecules and protein hydrogen atoms are omitted for clarity.

to protein, does not imply any kind of chemical bond but rather an affinity of a particular ion for the protein surface due to electrostatic and dispersion forces.

Firstly, the ion distribution around both proteins will be summarized. In choline chloride solution, choline shows certain affinity to the protein surface of BPTI and HRP. Despite the fact that both proteins are positively charged, there is practically no preferential binding of Cl^-. When choline is replaced by Na^+ a weak preference of ions for the BPTI surface is found. Sodium cations show also affinity to HRP surface, however the preference is much smaller than the preference for choline.

When sulfate is used as a counterion, the situation changes dramatically. For solution with choline, the choline peak remains unchanged. Sulfate shows a very strong preference for the protein surface. In sodium sulfate solution, sodium shows a weak preference for the surface.

We also carried out simulations of the mixture of sodium sulfate and choline chloride. The results indicate that it behaves like a superposition of individual salt solutions. For BPTI, the sulfate signal is the strongest. Sodium and choline show similar preference for the protein interface. For chloride, again no strong chloride affinity to the protein was found. The situation is slightly different in the case of HRP. Sulfate still shows very high affinity. However, sodium cations have the highest preference in this case.

Choline cations were found to favor interaction with negatively charged residues (Asp, Glu) but also nonspecifically with Arg, Cys, Gln, Gly, Leu, Met, Pro, Phe, Ser or Tyr amino acids. Sodium cation showed some preference for Asp, Asn, Glu, and Gln. On average, choline spends longer time than sodium in the vicinity of the protein, but without strong

amino acid specificity.

For chloride, very weak preference for positively charged Arg and Lys residues is found. Also, consistently with the ion distribution analysis, chlorides do not spend extended periods of time in the vicinity of the protein. Sulfate on the other hand exhibits very strong and long contacts with positively charged aminoacid residues. Sulfates are also often found to be bound in a kind of binding 'pockets', consistently with the literature.[122]

It can be concluded from the previous paragraphs, that ions have tendency to bind individually and independently of the other ions to specific sites at the protein surface. This can be clearly seen on the representative snapshots from the simulations, displayed in Fig. 4.1. Anions prefer positively charged sites, cations prefer negatively charged residues. For choline, there is also an affinity to hydrophobic residues, probably due to its partially hydrophobic character. In this respect, the ion–protein interactions resemble more the bulk interaction between charged species than interactions between ions and (charged) surfaces. Therefore, applicability of the ion–surface interaction models for proteins is rather questionable.

From our study of the same ions at the air/water interface[17] (Section 2.2.5) it turns out that the ion distributions are significantly different from those for the solution/protein interface. Chloride prefers the interface, whereas choline is weakly repelled from the interface. Sodium and sulfate clearly prefer bulk solvation. Thus, the relative surface preferences are reversed.

The influence of the different ions on the enzymatic activity could not be fully rationalized using the simulation data. However, some important conclusions can be drawn. Namely, the solution/protein interface cannot be viewed as an interface between a high dielectric and low dielectric media, since the solute behavior is dictated by local interactions between ions and individual protein residues. From this perspective, the use of the simplified surface model[128] is questionable. Sulfate is found to bind strongly to the proteins (to positively charged residues), however its effect on the enzymatic activity comes mainly from the solution pH change.[67] Choline that has an antagonistic role when compared to sulfate binds (among others) to hydrophobic residues, that can be found in the vicinity of the active site. In this way it can modify the activity of the enzyme.

4.2.2 Quantification and rationalization of the higher affinity of sodium over potassium to protein surface

This study[17] concerned the two most abundant monovalent cations in living organisms, sodium and potassium. They possess the same charge, and differ only slightly in their radii. Na^+ has a smaller ionic radius, but a higher hydrated radius than K^+.[131] According to Hofmeister[55] sodium destabilizes (salts out) hen's egg white protein more efficiently than potassium. Similar behavior was found also for other proteins.[132] Low intracellular and high extracellular Na^+/K^+ ratio maintained in living organisms by ion pumps shows the vital biological relevance of these ions.

We attempted to rationalize and quantify the different affinities of sodium and potassium to protein surfaces using MD simulations, quantum mechanical (QM) calculations and also conductivity measurements. The primitive solvation methods, still widely used to describe solvation of biomolecules, cannot distinguish between sodium and potassium. Therefore, their ion specificity has been to a large extent ignored.[133] Most of the calculations concering the interaction of ions with biomolecules are focused on polyvalent species possessing special biological functions. On the other hand Na^+ and K^+ are often viewed as merely defining the ionic strength of the solution. Our results for these ions, therefore, provide a new and highly relevant information about this biologically and biochemically interesting topic.

In this study, we systematically investigated the behavior of sodium and potassium at protein surfaces. We simulated five different proteins in aqueous mixtures of NaCl and KCl. Namely we studied actin (extracellular structural protein), BPTI (extracellular enzyme inhibiting protein), ubiquitin (intracellular protein marker), rubredoxin (intracellular electron transfer protein), and ribonuclease A (RNase A, intracellular model enzyme). We also performed conductivity measurements of RNase A and bovine serum albumin (BSA) in aqueous solutions of NaCl and KCl. To further rationalize the results we also performed MD simulations of solvated oligopeptides and isolated amino acids as well as QM calculations of ion pairing of alkali cations with small carboxylate ions (formate and acetate).

The principal results from the MD simulations are summarized in Figure 4.2, showing distribution functions and cumulative sums for both ions around the studied proteins. A cumulative sum (integrated distribution function) gives the average number of ions within a given distance of the protein. All curves show a higher affinity of Na^+ than K^+ to the protein, that can be attributed mainly to the effect of the carboxylate groups of Asp and Glu amino acid residues. The effect of backbone and particularly other functional groups is much weaker. Quantitatively, there are approximately twice as many Na^+ than K^+ ions near the protein surface and this is revealed as a generic property among all investigated proteins, despite their different structure and function.

The conductivity measurements of NaCl and KCl solutions with added proteins (RNase A and BSA) support these findings. We observed relative decrease in conductivity of the salt solution after addition of the protein. A larger decrease in the case of sodium salt indicated that Na^+ cations were more effectively removed from the solution to the protein surface than K^+ cations.

Specific ion effects at protein surfaces are often rationalized by means of surface tension changes caused by the presence of a given salt.[123,134,135] The analogy between air/water and protein/water interfaces could be good for the exposed hydrophobic patches of the protein with low dielectric constant. However, this description fails for the polar or charged hydrophilic parts that form the majority of the protein surface. Also, the ion–specific effects at the air/water interface are much stronger for anions than for cations, the latter being almost negligible.[136] The failure of the 'interfacial' model for proteins is consistent with the present picture showing the importance of the individual specific ion–amino acid interactions.[16,17] In this respect, the higher affinity of sodium over potassium to the protein

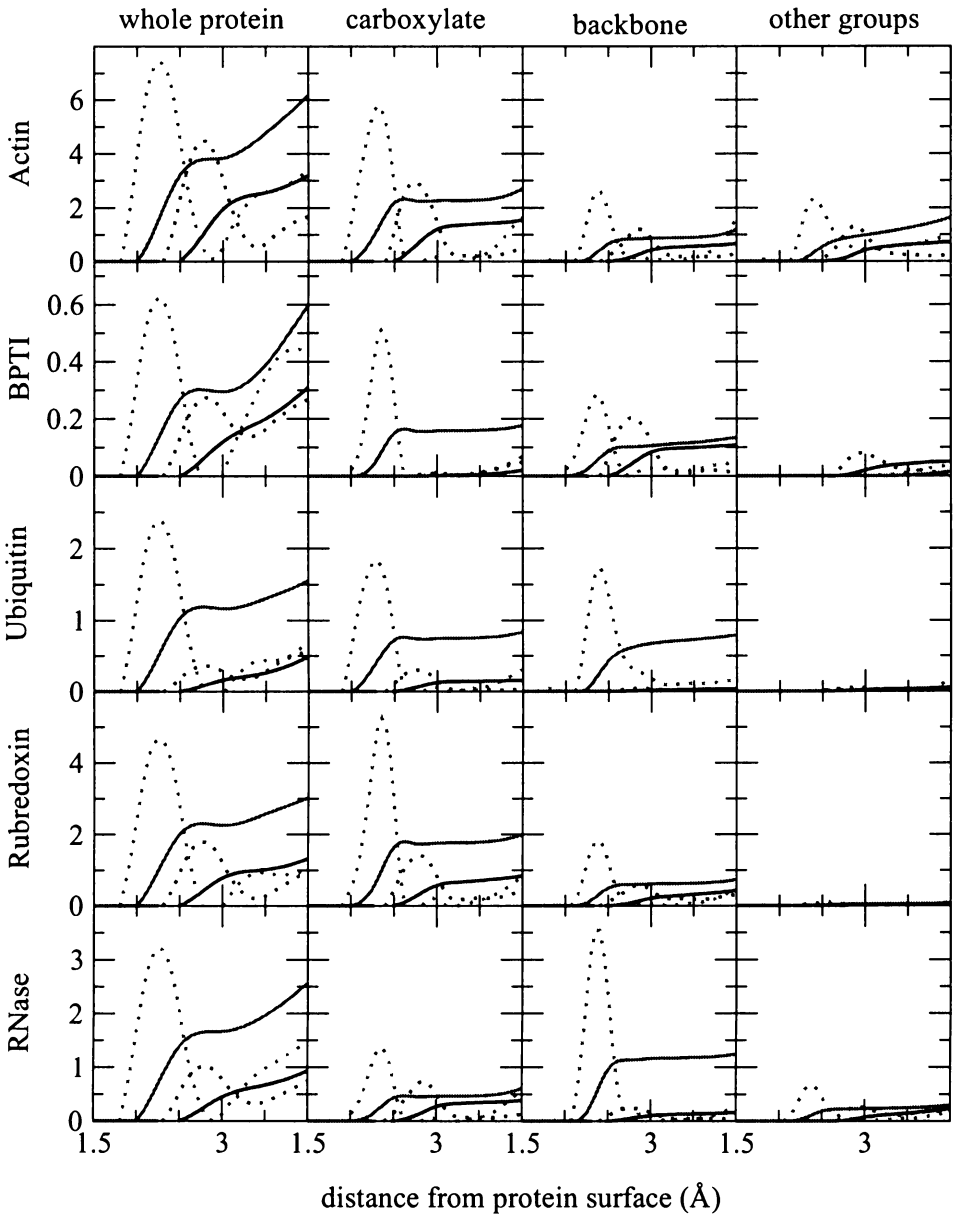

Figure 4.2: Distribution functions (dotted lines) and cumulative sums (solid lines) of cations around the five studied proteins. The cumulative sums give the average number of ions within a given distance from the protein surface. Results for the whole protein, carboxylate groups of the Asp and Glu aminoacids, backbone carbonyl group, and other side chain functional groups.

interface can be assigned to specific interaction with carboxylate groups in the protein side chains and the amide oxygens of the backbone.

This conclusion was further verified by MD simulations of solvated oligopeptides and isolated amino acids containing in the side chain carboxylate group (*i.e.*, aspartate and glu-

tamate). The possible effect of N- and C-terminal charged groups was eliminated by termination using the acetyl and N-methylamino groups. Consistent with the simulations of proteins, these cations reveal the Na^+/K^+ ratio of two to four. This relative preference is found both at the side chains and near the backbone. The former, representing ion–ion interaction is more important compared to the latter being weaker ion–dipole interaction of ion with the amide carbonyl group.

Simulation of acetate in the mixture of sodium, potassium and chloride ions showed a clear preference of Na^+ over K^+ by a factor of 3.4. QM calculations of pairing of sodium and potassium with formate and acetate, employing a polarizable continuum model for water,[137,138] showed that the pairing with Na^+ was favored by > 2 kcal/mol for both anions. This value suggests an even stronger preference of sodium for the carboxylate group. Similar calculations with formaldehyde (being a model system for the interactions with protein backbone) show a free energy preference of sodium of 1 kcal/mol. These results support the MD results concerning the ion specificity and selectivity at both protein sidechain and protein backbone.

Our results provide a clear and quantitative picture of the preference of sodium over potassium for protein surfaces, rationalized in terms of local cation–specific interactions with the carboxylate groups of Asp and Glu amino acid side chains. Additional contribution comes from the interactions with backbone amide carbonyl groups and to a smaller extent from other side chain groups. The results provide a new way to molecular understanding of many ion–specific phenomena involving protein interactions in salt solutions.

4.3 Further studies

The alkali cation – protein interactions play very important role in living organisms, *e.g.*, in protein folding or build up of protein functional networks.[139,140] The hydrophilic parts of proteins (where also the cations can bind) are often involved in protein–protein interactions within numerous intracellular and extracellular processes.[141,142] Further study of these interactions (and how they are influenced by various ions) can, therefore, have a far reaching impact in biochemistry and biotechnology. The obvious extension of this topic, being addressed presently, is a systematic study of affinity of different anions to protein surfaces, building on our previous knowledge.[16,17]

Chapter 5

Summary

This thesis consists of ten papers, where we investigated the properties of ions at various aqueous interfaces using methods of molecular dynamics simulations with polarizable or nonpolarizable potentials.

The largest part of the thesis is represented by publications[8–14] concerning the solvation properties of various organic and inorganic ions at the air/water interface. According to the classical picture,[30,31] simple inorganic ions (*e.g.*, halides) are repelled from the interface due to image forces. However, it has been shown that some ions show an appreciable propensity for the interface. This fact is discussed in the first paper.[10] Small and nonpolarizable ions like fluoride or alkali cations behave according to the classical picture. Large and polarizable inorganic ions (heavier halides), but also some molecular ions with large polarizability (azide and thiocyanate) can overcome the desolvation penalty caused by the transfer to the interface by polarization interactions. The presence of inorganic ions at the air/water interface has important consequences for several technological and atmospherical processes.[2,84]

Another class of ions – tetraalkylammonium cations – exhibit affinity to the interface due to their size and hydrophobicity. Both hydrophobicity and affinity to the interface increase with the increasing length of the alkyl chains. Tetramethylammonium, was found to be repelled from the interface and to prefer bulk solvation. Tetraethylammonium shows an intermediate behavior. Tetrapropyl– and tetrabutylammonium clearly behave as ionic surfactants.[12]

In three publications[8,9,11] we studied the counterion effects on aqueous solutions of TBA. Positive charge density due to adsorbed surfactant molecules at the surface was found to increase the already pronounced propensity of polarizable anions for the air/water interface. On the other hand, nonpolarizable fluoride anion tends to increase the amount of TBA cations in the bulk phase. Although polarization interactions were found to be important mainly for the proper description of soft anions, they also play some role for the description of solutions of nonpolarizable species, where the water polarization is an important contribution.

We also studied solvation properties of four biologically relevant ions (sodium, chloride, choline, and sulfate) at the air/water interface. Behind this study, there was our interest in the effect of these ions on the enzymatic activity of horseradish peroxidase.[16] Sodium and sulfate ions are repelled from the interface. Chloride exhibits certain surface affinity. The behavior of choline is dependent on the counteranion. With sulfate, it prefers bulk solvation, with chloride it has appreciable affinity for the subsurface. This is in striking contrast with the properties of these ions in the vicinity of proteins[16] (see below).

Simulations of ionic (DMP) and zwitterionic (DPN) surfactants[13] confirmed their strong adsorption at the interface. For the ionic species, the bromide counterions mostly co–adsorb to the surface, however, they are also present in the bulk phase. After addition of KBr and KF to the simulation cell, the effects of additional ions were addressed. KF does not strongly affect neither DMP nor DPN. On the other hand, strong surface propensity of bromide results in sizable effects on ionic distribution at the interface. The findings are consistent with the results of VSFG and SHG measurements reported in this joint publication.

In our study of interior and interfacial solvation of benzene dicarboxylate ions, carried out in cooperation with experimental laboratory measuring PES spectra of these species, we concentrated on the properties of *o*-, *m*-, and *p*-benzene dicarboxylates.[14] All three species were found to prefer bulk solvation due to their double negative charge. After tetramethylation of the ortho isomer, the hydrophobicity overwhelms the electrostatic interactions and the dicarboxylate anion solvates at the interface. A strong orientational preference is found for this substance, with carboxylates anchored in the subsurface layer and the benzene ring laying on the water surface.

In the second part of the thesis results of computer simulations of brine rejection from freezing salt solutions are reported.[15] Our group was the first one which succesfully simulated this very important natural process in a computer. After establishing a robust protocol for reproducible freezing of water using MD simulations, we were able to observe the brine rejection. According to the results we proposed a mechanism for this process where the local fluctuation (decrease) in salt concentration is accompanied by a buildup of a new ice layer. At the end of the simulation, almost the whole simulation cell is frozen with the exception of a thin slice of unfrozen brine.

Last two publications[16,17] focus on ion interactions with proteins, and discuss whether their surfaces can be taken as an example of an interface. The first study[16] was motivated by the experimental observation that some ions (sulfate) can induce superactivity in the horseradish peroxidase by the pH changes of the solution, whereas others (choline) have antagonistic behavior that could not be described by pH changes only. MD simulations indicate that both choline and sulfate have a large affinity to the protein, but bind to very different regions. Sulfate prefers solvent exposed positively charged residues. Choline, in addition to its interaction with negatively charged amino acids, shows also preference for hydrophobic residues that can be found close to the active site. Choline induced decrease of activity can be therefore assigned to its affinity to the regions of the protein responsible

for the enzymatic reaction. It also emerges from this study that interactions of ions with proteins have a local and specific character. Their proper description requires the use of individual ion–aminoacid interactions, rather than some kind of an averaged ion–surface framework.

The local and specific character of ion–protein interactions is confirmed in our study of preferential adsorption of Na^+ versus K^+ to protein surfaces.[17] The two to fourfold enhancement of sodium over potassium emerging from the MD simulations of proteins in salt solutions can be assigned to its preferrential pairing with carboxylate groups of Asp and Glu aminoacids, to carbonyl oxygens of the backbone amide groups, and to a much smaller extent also to interactions with other functional groups. Simulations of short oligopeptides and isolated amino acids, and QM calculations of ion pairing with carboxylate functional group (represented by formate and acetate) comfirm the preference of sodium near the protein surface. The experimental observations of the change in the conductivity of NaCl or KCl solutions upon addition of proteins also show that the sodium is more effectively removed from the solution by adsorption on the protein.

To summarize, in this work we attempted to demonstrate the applicability of methods of molecular dynamics to a wide scale of problems pertinent to the properties of ions at interfaces. Due to the fact that ions are ubiquitous our results provide information relevant for many different fields, *e.g.*, for atmospheric chemistry, biochemistry and biology, or technology.

References

[1] B. J. Finlayson-Pitts, "The tropospheric chemistry of sea salt: A molecular-level view of the chemistry of NaCl and NaBr", *Chemical Reviews* **103**(12), pp. 4801–4822 (2003).

[2] E. M. Knipping, M. J. Lakin, K. L. Foster, P. Jungwirth, D. J. Tobias, R. B. Gerber, D. Dabdub, and B. J. Finlayson-Pitts, "Experiments and simulations of ion-enhanced interfacial chemistry on aqueous NaCl aerosols", *Science* **288**(5464), pp. 301–306 (2000).

[3] A. Y. Shcherbina, L. D. Talley, and D. L. Rudnick, "Direct observations of North Pacific ventilation: Brine rejection in the Okhotsk Sea", *Science* **302**(5652), pp. 1952–1955 (2003).

[4] P. Kritzer, "Corrosion in high-temperature and supercritical water and aqueous solutions: a review", *Journal of Supercritical Fluids* **29**(1), pp. 1–29 (2004).

[5] M. G. Cacace, E. M. Landau, and J. J. Ramsden, "The Hofmeister series: salt and solvent effects on interfacial phenomena", *Quarterly Reviews of Biophysics* **30**(3), pp. 241–277 (1997).

[6] M. Gradzielski, "Investigations of the dynamics of morphological transitions in amphiphilic systems", *Current Opinion In Colloid & Interface Science* **9**(3), pp. 256–263 (2004).

[7] A. Corma, "State of the art and future challenges of zeolites as catalysts", *Journal of Catalysis* **216**(1), pp. 298–312 (2003).

[8] B. Winter, R. Weber, P. M. Schmidt, I. V. Hertel, M. Faubel, L. Vrbka, and P. Jungwirth, "Molecular structure of surface-active salt solutions: Photoelectron spectroscopy and molecular dynamics simulations of aqueous tetrabutylammonium iodide", *Journal of Physical Chemistry B* **108**(38), pp. 14558–14564 (2004).

[9] B. Winter, R. Weber, I. V. Hertel, M. Faubel, L. Vrbka, and P. Jungwirth, "Effect of bromide on the interfacial structure of aqueous tetrabutylammonium iodide: Photoelectron spectroscopy and molecular dynamics simulations", *Chemical Physics Letters* **410**(4), pp. 222–227 (2005).

[10] L. Vrbka, M. Mucha, B. Minofar, P. Jungwirth, E. C. Brown, and D. J. Tobias, "Propensity of soft ions for the air/water interface", *Current Opinion In Colloid & Interface Science* **9**(1), pp. 67–73 (2004).

[11] L. Vrbka and P. Jungwirth, "Counter-ion effects and interfacial properties of aqueous tetrabutylammonium halide solutions", *Australian Journal of Chemistry* **57**(12), pp. 1211–1217 (2004).

[12] T. Hrobárik, L. Vrbka, and P. Jungwirth, "Selected biologically relevant ions at the air/water interface: A comparative molecular dynamics study", *Biophysical Chemistry* **124**(3), pp. 238–242 (2006).

[13] M. Petrov, B. Minofar, L. Vrbka, P. Jungwirth, P. Koelsch, and H. Motschmann, "Aqueous ionic and complementary zwitterionic soluble surfactants: Molecular dynamics simulations and sum frequency generation spectroscopy of the surfaces", *Langmuir* **22**(6), pp. 2498–2505 (2006).

[14] B. Minofar, L. Vrbka, M. Mucha, P. Jungwirth, X. Yang, X. B. Wang, Y. J. Fu, and L. S. Wang, "Interior and interfacial aqueous solvation of benzene dicarboxylate dianions and their methylated analogues: A combined molecular dynamics and photoelectron spectroscopy study", *Journal of Physical Chemistry A* **109**(23), pp. 5042–5049 (2005).

[15] L. Vrbka and P. Jungwirth, "Brine rejection from freezing salt solutions: A molecular dynamics study", *Physical Review Letters* **95**(14), pp. 148501 (2005).

[16] L. Vrbka, P. Jungwirth, P. Bauduin, D. Touraud, and W. Kunz, "Specific ion effects at protein surfaces: A molecular dynamics study of bovine pancreatic trypsin inhibitor and horseradish peroxidase in selected salt solutions", *Journal of Physical Chemistry B* **110**(13), pp. 7036–7043 (2006).

[17] L. Vrbka, J. Vondrášek, B. Jagoda-Ćwiklik, R. Vácha, and P. Jungwirth, "Quantification and rationalization of the higher affinity of sodium over potassium to protein surfaces", *Proceedings of The National Academy of Sciences of The United States of America* **103**(42), pp. 15440–15444 (2006).

[18] M. P. Allen and D. J. Tildesley, *Computer simulations of liquids*, Oxford University Press (1987).

[19] A. R. Leach, *Molecular modelling, principles and applications*, Pearson Education Limited (2001).

[20] D. Frenkel and B. Smit, *Understanding molecular simulation*, Academic Press (2002).

[21] P. M. Morse, "Diatomic molecules according to the wave mechanics. II. Vibrational levels", *Physical Reviews* **34**, pp. 57–64 (1929).

[22] B. T. Thole, "Molecular polarizabilities calculated with a modified dipole interaction", *Chemical Physics* **59**(3), pp. 341–350 (1981).

[23] M. Mucha, "Modeling of structure and dynamics of liquid clusters and surfaces", doctoral thesis (2006).

[24] P. B. Petersen, R. J. Saykally, M. Mucha, and P. Jungwirth, "Enhanced concentration of polarizable anions at the liquid water surface: SHG spectroscopy and MD simulations of sodium thiocyanate", *Journal of Physical Chemistry B* **109**(21), pp. 10915–10921 (2005).

[25] T. Darden, D. York, and L. Pedersen, "Particle mesh Ewald - an n.log(n) method for Ewald sums in large systems", *Journal of Chemical Physics* **98**(12), pp. 10089–10092 (1993).

[26] U. Essmann, L. Perera, M. L. Berkowitz, T. Darden, H. Lee, and L. G. Pedersen, "A smooth particle mesh Ewald method", *Journal of Chemical Physics* **103**(19), pp. 8577–8593 (1995).

[27] B. A. Luty, I. G. Tironi, and W. F. van Gunsteren, "Lattice-sum methods for calculating electrostatic interactions in molecular simulations", *Journal of Chemical Physics* **103**(8), pp. 3014–3021 (1995).

[28] E. Spohr, "Effect of electrostatic boundary conditions and system size on the interfacial properties of water and aqueous solutions", *Journal of Chemical Physics* **107**(16), pp. 6342–6348 (1997).

[29] I. C. Yeh and M. L. Berkowitz, "Ewald summation for systems with slab geometry", *Journal of Chemical Physics* **111**(7), pp. 3155–3162 (1999).

[30] C. Wagner, "The surface tension of dilute solutions of electrolytes", *Physikalische Zeitschrift* **25**, pp. 474–477 (1924).

[31] L. Onsager and N. T. Samaras, "The surface tension of Debye–Hüeckel electrolytes", *Journal of Chemical Physics* **2**, pp. 528–536 (1934).

[32] M. A. Wilson and A. Pohorille, "Interaction of monovalent ions with the water liquid vapor interface - A molecular-dynamics study", *Journal of Chemical Physics* **95**(8), pp. 6005–6013 (1991).

[33] I. Benjamin, "Theoretical-study of ion solvation at the water liquid-vapor interface", *Journal of Chemical Physics* **95**(5), pp. 3698–3709 (1991).

[34] P. Jungwirth and D. J. Tobias, "Ions at the air/water interface", *Journal of Physical Chemistry B* **106**(25), pp. 6361–6373 (2002).

[35] M. J. Shultz, S. Baldelli, C. Schnitzer, and D. Simonelli, "Aqueous solution/air interfaces probed with sum frequency generation spectroscopy", *Journal of Physical Chemistry B* **106**(21), pp. 5313–5324 (2002).

[36] P. B. Petersen, J. C. Johnson, K. P. Knutsen, and R. J. Saykally, "Direct experimental validation of the Jones-Ray effect", *Chemical Physics Letters* **397**(1), pp. 46–50 (2004).

[37] P. Jungwirth and D. J. Tobias, "Specific ion effects at the air/water interface", *Chemical Reviews* **106**(4), pp. 1259–1281 (2006).

[38] L. Perera and M. L. Berkowitz, "Many-body effects in molecular-dynamics simulations of $Na^+(H_2O)_n$ and $Cl^-(H_2O)_n$ clusters", *Journal of Chemical Physics* **95**(3), pp. 1954–1963 (1991).

[39] L. Perera and M. L. Berkowitz, "Stabilization energies of Cl^-, Br^-, and I^- ions in water clusters", *Journal of Chemical Physics* **99**(5), pp. 4222–4224 (1993).

[40] L. Perera and M. L. Berkowitz, "Structures of $Cl^-(H_2O)_n$ and $F^-(H_2O)_n$ (n=2,3,...,15) clusters - molecular-dynamics computer-simulations", *Journal of Chemical Physics* **100**(4), pp. 3085–3093 (1994).

[41] L. X. Dang and B. C. Garrett, "Photoelectron-spectra of the hydrated iodine anion from molecular-dynamics simulations", *Journal of Chemical Physics* **99**(4), pp. 2972–2977 (1993).

[42] D. Hagberg, S. Brdarski, and G. Karlstrom, "On the solvation of ions in small water droplets", *Journal of Physical Chemistry B* **109**(9), pp. 4111–4117 (2005).

[43] G. Markovich, S. Pollack, R. Giniger, and O. Cheshnovsky, "Photoelectron-spectroscopy of Cl^-, Br^-, and I^- solvated in water clusters", *Journal of Chemical Physics* **101**(11), pp. 9344–9353 (1994).

[44] J. H. Choi, K. T. Kuwata, Y. B. Cao, and M. Okumura, "Vibrational spectroscopy of the $Cl^-(H_2O)_n$ anionic clusters, n=1-5", *Journal of Physical Chemistry A* **102**(3), pp. 503–507 (1998).

[45] S. S. Xantheas, "Quantitative description of hydrogen bonding in chloride-water clusters", *Journal of Physical Chemistry* **100**(23), pp. 9703–9713 (1996).

[46] D. J. Tobias, P. Jungwirth, and M. Parrinello, "Surface solvation of halogen anions in water clusters: An ab initio molecular dynamics study of the $Cl^-(H_2O)_6$ complex", *Journal of Chemical Physics* **114**(16), pp. 7036–7044 (2001).

[47] R. Ayala, J. M. Martinez, R. R. Pappalardo, and E. S. Marcos, "Study of the stabilization energies of halide-water clusters: An application of first-principles interaction potentials based on a polarizable and flexible model", *Journal of Chemical Physics* **121**(15), pp. 7269–7275 (2004).

[48] P. Salvador, J. E. Curtis, D. J. Tobias, and P. Jungwirth, "Polarizability of the nitrate anion and its solvation at the air/water interface", *Physical Chemistry Chemical Physics* **5**(17), pp. 3752–3757 (2003).

[49] X. Yang, B. Kiran, X. B. Wang, L. S. Wang, M. Mucha, and P. Jungwirth, "Solvation of the azide anion (n_3^-) in water clusters and aqueous interfaces: A combined investigation by photoelectron spectroscopy, density functional calculations, and molecular dynamics simulations", *Journal of Physical Chemistry A* **108**(39), pp. 7820–7826 (2004).

[50] S. J. Stuart and B. J. Berne, "Surface curvature effects in the aqueous ionic solvation of the chloride ion", *Journal of Physical Chemistry A* **103**(49), pp. 10300–10307 (1999).

[51] P. Jungwirth and D. J. Tobias, "Surface effects on aqueous ionic solvation: A molecular dynamics simulation study of NaCl at the air/water interface from infinite dilution to saturation", *Journal of Physical Chemistry B* **104**(32), pp. 7702–7706 (2000).

[52] P. Jungwirth and D. J. Tobias, "Molecular structure of salt solutions: A new view of the interface with implications for heterogeneous atmospheric chemistry", *Journal of Physical Chemistry B* **105**(43), pp. 10468–10472 (2001).

[53] P. Jungwirth, J. E. Curtis, and D. J. Tobias, "Polarizability and aqueous solvation of the sulfate dianion", *Chemical Physics Letters* **367**(5), pp. 704–710 (2003).

[54] A. Heydweiller, "Über physikalische Eigenschaften von Lösungen in ihrem Zusammenhang. II. Oberflächenspannung und elektrisches Leitvermögen wässeriger Salzlösungen", *Annalen der Physik* **338**(11), pp. 145–185 (1910).

[55] F. Hofmeister, "Zur Lehre von der Wirkung der Salze", *Archiv für experimentelle Pathologie und Pharmakologie* **24**, pp. 247 (1888).

[56] R. Defay, I. Prigogine, and A. Bellemans, *Surface tension and adsorption*, London: Longmans Green (1966).

[57] R. Moberg, F. Bökman, O. Bohman, and H. O. G. Siegbahn, "ESCA studies of phase-transfer catalysts in solution - ion-pairing and surface-activity", *Journal of The American Chemical Society* **113**(10), pp. 3663–3667 (1991).

[58] R. Weber, B. Winter, P. M. Schmidt, W. Widdra, I. V. Hertel, M. Dittmar, and M. Faubel, "Photoemission from aqueous alkali-metal-iodide salt solutions using EUV synchrotron radiation", *Journal of Physical Chemistry B* **108**(15), pp. 4729–4736 (2004).

[59] S. Holmberg, Z. C. Yuan, R. Moberg, and H. Siegbahn, "Surface segregation of tetra-n-alkylammonium halides in formamide investigated by angle resolved electron-spectroscopy", *Journal of Electron Spectroscopy and Related Phenomena* 47 , pp. 27–38 (1988).

[60] L. X. Dang and T. M. Chang, "Molecular mechanism of ion binding to the liquid/vapor interface of water", *Journal of Physical Chemistry B* **106**(2), pp. 235–238 (2002).

[61] H. Morgner, J. Oberbrodhage, K. Richter, and K. Roth, "The solution of tetrabutylammoniumiodide in formamide - investigation of the surface by MIES", *Journal of Physics-condensed Matter* **3**(29), pp. 5639–5655 (1991).

[62] F. Eschen, M. Heyerhoff, H. Morgner, and J. Vogt, "The concentration-depth profile at the surface of a solution of tetrabutylammonium iodide in formamide, based on angle-resolved photoelectron-spectroscopy", *Journal of Physics-condensed Matter* **7**(10), pp. 1961–1978 (1995).

[63] G. Andersson and H. Morgner, "Investigations on solutions of tetrabutylonium salts in formamide with NICISS and ICISS: concentration depth profiles and composition of the outermost layer", *Surface Science* **445**(1), pp. 89–99 (2000).

[64] V. B. Luzhkov and J. Aqvist, "Mechanisms of tetraethylammonium ion block in the KcsA potassium channel", *Febs Letters* **495**(3), pp. 191–196 (2001).

[65] E. Kutluay, B. Roux, and L. Heginbotham, "Rapid intracellular TEA block of the KcsA potassium channel", *Biophysical Journal* **88**(2), pp. 1018–1029 (2005).

[66] T. I. Morrow and E. J. Maginn, "Density, local composition and diffusivity of aqueous choline chloride solutions: A molecular dynamics study", *Fluid Phase Equilibria* **217**(1), pp. 97–104 (2004).

[67] M. C. Pinna, P. Bauduin, D. Touraud, M. Monduzzi, B. W. Ninham, and W. Kunz, "Hofmeister effects in biology: Effect of choline addition on the salt-induced super activity of horseradish peroxidase and its implication for salt resistance of plants", *Journal of Physical Chemistry B* **109**(34), pp. 16511–16514 (2005).

[68] P. Kölsch and H. Motschmann, "Varying the counterions at a charged interface", *Langmuir* **21**(8), pp. 3436–3442 (2005).

[69] K. Kawamura, L. L. Ng, and I. R. Kaplan, "Determination of organic-acids (C1-C10) in the atmosphere, motor exhausts, and engine oils", *Environmental Science & Technology* **19**(11), pp. 1082–1086 (1985).

[70] K. Kawamura, N. Umemoto, M. Mochida, T. Bertram, S. Howell, and B. J. Huebert, "Water-soluble dicarboxylic acids in the tropospheric aerosols collected over east Asia and western North Pacific by ACE-Asia C-130 aircraft", *Journal of Geophysical Research - Atmospheres* **108**(D23), pp. 8639 (2003).

[71] V. M. Kerminen, C. Ojanen, T. Pakkanen, R. Hillamo, M. Aurela, and J. Merilainen, "Low-molecular-weight dicarboxylic acids in an urban and rural atmosphere", *Journal of Aerosol Science* **31**(3), pp. 349–362 (2000).

[72] V. M. Kerminen, "Relative roles of secondary sulfate and organics in atmospheric cloud condensation nuclei production", *Journal of Geophysical Research - Atmospheres* **106**(15), pp. 17321–17333 (2001).

[73] J. H. Seinfeld and J. F. Pankow, "Organic atmospheric particulate material", *Annual Review of Physical Chemistry 54* , pp. 121–140 (2003).

[74] X. Yang, Y. J. Fu, X. B. Wang, P. Slavicek, M. Mucha, P. Jungwirth, and L. S. Wang, "Solvent-mediated folding of a doubly charged anion", *Journal of The American Chemical Society* **126**(3), pp. 876–883 (2004).

[75] B. Minofar, M. Mucha, P. Jungwirth, X. Yang, Y. J. Fu, X. B. Wang, and L. S. Wang, "Bulk versus interfacial aqueous solvation of dicarboxylate dianions", *Journal of The American Chemical Society* **126**(37), pp. 11691–11698 (2004).

[76] I. F. W. Kuo and C. J. Mundy, "An ab initio molecular dynamics study of the aqueous liquid-vapor interface", *Science* **303**(5658), pp. 658–660 (2004).

[77] I. F. W. Kuo, C. J. Mundy, B. L. Eggimann, M. J. McGrath, J. I. Siepmann, B. Chen, J. Vieceli, and D. J. Tobias, "Structure and dynamics of the aqueous liquid-vapor interface: A comprehensive particle-based simulation study", *Journal of Physical Chemistry B* **110**(8), pp. 3738–3746 (2006).

[78] C. J. Mundy and I. F. W. Kuo, "First-principles approaches to the structure and reactivity of atmospherically relevant aqueous interfaces", *Chemical Reviews* **106**(4), pp. 1282–1304 (2006).

[79] V. F. Petrenko and R. W. Whitworth, *Physics of ice*, Oxford University Press (1999).

[80] R. E. Dickerson, *Molecular thermodynamics*, W. A. Benjamin, Pasadena (1969).

[81] B. Rubinsky, "Solidification processes in saline solutions", *Journal of Crystal Growth* **62**(3), pp. 513–522 (1983).

[82] M. G. Worster and J. S. Wettlaufer, "Natural convection, solute trapping, and channel formation during solidification of saltwater", *Journal of Physical Chemistry B* **101**(32), pp. 6132–6136 (1997).

[83] W. W. Mullins and R. F. Sekerka, "Stability of a planar interface during solidification of a dilute binary alloy", *Journal of Applied Physics* **32**(2), pp. 444–451 (1964).

[84] P. Jungwirth, D. Rosenfeld, and V. Buch, "A possible new molecular mechanism of thundercloud electrification", *Atmospheric Research* **76**(1), pp. 190–205 (2005).

[85] K. Nagashima and Y. Furukawa, "Time development of a solute diffusion field and morphological instability on a planar interface in the directional growth of ice crystals", *Journal of Crystal Growth* **209**(1), pp. 167–174 (2000).

[86] I. M. Svishchev and P. G. Kusalik, "Electrofreezing of liquid water: A microscopic perspective", *Journal of The American Chemical Society* **118**(3), pp. 649–654 (1996).

[87] B. Guillot, "A reappraisal of what we have learnt during three decades of computer simulations on water", *Journal of Molecular Liquids* **101**(1), pp. 219–260 (2002).

[88] C. Vega, E. Sanz, and J. L. F. Abascal, "The melting temperature of the most common models of water", *Journal of Chemical Physics* **122**(11), pp. 114507 (2005).

[89] H. J. C. Berendsen, J. R. Grigera, and T. P. Straatsma, "The missing term in effective pair potentials", *Journal of Physical Chemistry* **91**(24), pp. 6269–6271 (1987).

[90] T. Bryk and A. D. J. Haymet, "The ice/water interface: Density-temperature phase diagram for the SPC/e model of liquid water", *Molecular Simulation* **30**(2), pp. 131–135 (2004).

[91] T. Bryk and A. D. J. Haymet, "Charge separation at the ice/water interface: a molecular dynamics simulation study of solute ions at the ice basal plane", *Journal of Molecular Liquids* **112**(1), pp. 47–50 (2004).

[92] D. E. Smith and L. X. Dang, "Computer-simulations of NaCl association in polarizable water", *Journal of Chemical Physics* **100**(5), pp. 3757–3766 (1994).

[93] K. Morishige and H. Uematsu, "The proper structure of cubic ice confined in mesopores", *Journal of Chemical Physics* **122**(4), pp. 044711 (2005).

[94] E. Whalley, "Scheiners halo - evidence for ice Ic in the atmosphere", *Science* **211**(4480), pp. 389–390 (1981).

[95] E. Whalley, "Cubic ice in nature", *Journal of Physical Chemistry* **87**(21), pp. 4174–4179 (1983).

[96] B. J. Murray, D. A. Knopf, and A. K. Bertram, "The formation of cubic ice under conditions relevant to Earth's atmosphere", *Nature* **434**(7030), pp. 202–205 (2005).

[97] G. P. Johari, "Water's size-dependent freezing to cubic ice", *Journal of Chemical Physics* **122**(19), pp. 194504 (2005).

[98] T. Bryk and A. D. J. Haymet, "Ice 1h/water interface of the SPC/e model: Molecular dynamics simulations of the equilibrium basal and prism interfaces", *Journal of Chemical Physics* **117**(22), pp. 10258–10268 (2002).

[99] J. A. Hayward and A. D. J. Haymet, "The ice/water interface: Molecular dynamics simulations of the basal, prism, $20(2)\bar{1}$, and $2(11)\bar{0}$ interfaces of ice Ih", *Journal of Chemical Physics* **114**(8), pp. 3713–3726 (2001).

[100] H. Nada and Y. Furukawa, "Anisotropic growth kinetics of ice crystals from water studied by molecular dynamics simulation", *Journal of Crystal Growth* **169**(3), pp. 587–597 (1996).

[101] H. Nada and J. P. J. M. van der, "An intermolecular potential model for the simulation of ice and water near the melting point: A six-site model of H_2O", *Journal of Chemical Physics* **118**(16), pp. 7401–7413 (2003).

[102] H. Nada, J. P. van der, and Y. Furukawa, "A clear observation of crystal growth of ice from water in a molecular dynamics simulation with a six-site potential model of H_2O", *Journal of Crystal Growth* **266**(1), pp. 297–302 (2004).

[103] M. A. Carignano, P. B. Shepson, and I. Szleifer, "Molecular dynamics simulations of ice growth from supercooled water", *Molecular Physics* **103**(21), pp. 2957–2967 (2005).

[104] A. Tabazadeh, Y. S. Djikaev, and H. Reiss, "Surface crystallization of supercooled water in clouds", *Proceedings of The National Academy of Sciences of The United States of America* **99**(25), pp. 15873–15878 (2002).

[105] M. Del Guasta, M. Morandi, L. Stefanutti, S. Balestri, E. Kyro, M. Rummukainen, R. Kivi, V. Rizi, B. Stein, C. Wedekind, B. Mielke, R. Matthey, V. Mitev, and M. Douard, "LIDAR observation of spherical particles in a -65 degrees cold cirrus observed above Sodankyla (Finland) during SESAME", *Journal of Aerosol Science* **29**(3), pp. 357–374 (1998).

[106] H. Prupacher and J. D. Klett, *Microphysics of Clouds and Precipitation*, Kluwer Academic Publishers, Dordrecht (1998).

[107] J. E. Kay, V. Tsemekhman, B. Larson, M. Baker, and B. Swanson, "Comment on evidence for surface-initiated homogeneous nucleation", *Atmospheric Chemistry and Physics 3* , pp. 1439–1443 (2003).

[108] D. Duft and T. Leisner, "Laboratory evidence for volume-dominated nucleation of ice in supercooled water microdroplets", *Atmospheric Chemistry and Physics 4* , pp. 1997–2000 (2004).

[109] R. A. Shaw, A. J. Durant, and Y. Mi, "Heterogeneous surface crystallization observed in undercooled water", *Journal of Physical Chemistry B* **109**(20), pp. 9865–9868 (2005).

[110] S. Sastry, "Water - Ins and outs of ice nucleation", *Nature* **438**(7069), pp. 746–747 (2005).

[111] B. B. Laird and A. D. J. Haymet, "The crystal liquid interface - structure and properties from computer-simulation", *Chemical Reviews* **92**(8), pp. 1819–1837 (1992).

[112] L. A. Baez and P. Clancy, "Phase-equilibria in extended simple point-charge ice-water systems", *Journal of Chemical Physics* **103**(22), pp. 9744–9755 (1995).

[113] H. Nada and Y. Furukawa, "Anisotropy in molecular-scaled growth kinetics at ice-water interfaces", *Journal of Physical Chemistry B* **101**(32), pp. 6163–6166 (1997).

[114] T. Ikeda-Fukazawa and K. Kawamura, "Molecular-dynamics studies of surface of ice Ih", *Journal of Chemical Physics* **120**(3), pp. 1395–1401 (2004).

[115] E. J. Smith, T. Bryk, and A. D. J. Haymet, "Free energy of solvation of simple ions: Molecular-dynamics study of solvation of Cl^- and Na^+ in the ice/water interface", *Journal of Chemical Physics* **123**(3), pp. 034706 (2005).

[116] K. Koga, G. T. Gao, H. Tanaka, and X. C. Zeng, "Formation of ordered ice nanotubes inside carbon nanotubes", *Nature* **412**(6849), pp. 802–805 (2001).

[117] R. Radhakrishnan and B. L. Trout, "Nucleation of hexagonal ice (Iho-h) in liquid water", *Journal of The American Chemical Society* **125**(25), pp. 7743–7747 (2003).

[118] M. Matsumoto, S. Saito, and I. Ohmine, "Molecular dynamics simulation of the ice nucleation and growth process leading to water freezing", *Nature* **416**(6879), pp. 409–413 (2002).

[119] M. Yamada, S. Mossa, H. E. Stanley, and F. Sciortino, "Interplay between time-temperature transformation and the liquid-liquid phase transition in water", *Physical Review Letters* **88**(19), pp. 195701 (2002).

[120] L. Vrbka and P. Jungwirth, "Homogeneous freezing of water starts in the subsurface", *Journal of Physical Chemistry B* **110**(37), pp. 18126–18129 (2006).

[121] K. D. Collins and M. W. Washabaugh, "The Hofmeister effect and the behavior of water at interfaces", *Quarterly Reviews of Biophysics* **18**(4), pp. 323–422 (1985).

[122] P. Chakrabarti, "Anion-binding sites in protein structures", *Journal of Molecular Biology* **234**(2), pp. 463–482 (1993).

[123] T. Arakawa and S. N. Timasheff, "Preferential interactions of proteins with salts in concentrated-solutions", *Biochemistry* **21**(25), pp. 6545–6552 (1982).

[124] S. N. Timasheff and T. Arakawa, "Mechanism of protein precipitation and stabilization by co-solvents", *Journal of Crystal Growth* **90**(1), pp. 39–46 (1988).

[125] T. Arakawa, R. Bhat, and S. N. Timasheff, "Why preferential hydration does not always stabilize the native structure of globular-proteins", *Biochemistry* **29**(7), pp. 1924–1931 (1990).

[126] T. Arakawa and S. N. Timasheff, "Theory of protein solubility", *Methods in Enzymology* **114**(part A), pp. 49–77 (1985).

[127] R. A. Curtis, J. M. Prausnitz, and H. W. Blanch, "Protein-protein and protein-salt interactions in aqueous protein solutions containing concentrated electrolytes", *Biotechnology and Bioengineering* **57**(1), pp. 11–21 (1998).

[128] M. Boström, D. R. M. Williams, and B. W. Ninham, "Special ion effects: Why the properties of lysozyme in salt solutions follow a Hofmeister series", *Biophysical Journal* **85**(2), pp. 686–694 (2003).

[129] W. Kunz, L. Belloni, O. Bernard, and B. W. Ninham, "Osmotic coefficients and surface tensions of aqueous electrolyte solutions: Role of dispersion forces", *Journal of Physical Chemistry B* **108**(7), pp. 2398–2404 (2004).

[130] P. Bauduin, F. Nohmie, D. Touraud, R. Neueder, W. Kunz, and B. W. Ninham, "Hofmeister specific-ion effects on enzyme activity and buffer pH: Horseradish peroxidase in citrate buffer", *Journal of Molecular Liquids* **123**(1), pp. 14–19 (2006).

[131] E. R. Nightingale, "Phenomenological theory of ion solvation. Effective radii of hydrated ions", *Journal of Physical Chemistry* **63**(9), pp. 1381–1387 (1959).

[132] K. Inouye, K. Kuzuya, and B. Tonomura, "Effect of salts on the solubility of thermolysin: A remarkable increase in the solubility as well as the activity by the addition of salts without aggregation or dispersion of thermolysin", *Journal of Biochemistry* **123**(5), pp. 847–852 (1998).

[133] K. D. Collins, "Charge density-dependent strength of hydration and biological structure", *Biophysical Journal* **72**(1), pp. 65–76 (1997).

[134] K. D. Collins, "Ions from the Hofmeister series and osmolytes: effects on proteins in solution and in the crystallization process", *Methods* **34**(3), pp. 300–311 (2004).

[135] T. Y. Lin and S. N. Timasheff, "On the role of surface tension in the stabilization of globular proteins", *Protein Science* **5**(2), pp. 372–381 (1996).

[136] P. K. Weissenborn and R. J. Pugh, "Surface tension of aqueous solutions of electrolytes: Relationship with ion hydration, oxygen solubility, and bubble coalescence", *Journal of Colloid and Interface Science* **184**(2), pp. 550–563 (1996).

[137] V. Barone and M. Cossi, "Quantum calculation of molecular energies and energy gradients in solution by a conductor solvent model", *Journal of Physical Chemistry A* **102**(11), pp. 1995–2001 (1998).

[138] M. Cossi, N. Rega, G. Scalmani, and V. Barone, "Energies, structures, and electronic properties of molecules in solution with the C-PCM solvation model", *Journal of Computational Chemistry* **24**(6), pp. 669–681 (2003).

[139] S. Maldonado, M. P. Irun, L. A. Campos, J. A. Rubio, A. Luquita, A. Lostao, R. J. Wang, B. Garcia-Moreno, and J. Sancho, "Salt-induced stabilization of apoflavodoxin at neutral pH is mediated through canon-specific effects", *Protein Science* **11**(5), pp. 1260–1273 (2002).

[140] B. N. Dominy, D. Perl, F. X. Schmid, and C. L. Brooks, "The effects of ionic strength on protein stability: The cold shock protein family", *Journal of Molecular Biology* **319**(2), pp. 541–554 (2002).

[141] I. Muegge, T. Schweins, and A. Warshel, "Electrostatic contributions to protein-protein binding affinities: Application to Rap/Raf interaction", *Proteins-structure Function and Bioinformatics* **30**(4), pp. 407–423 (1998).

[142] R. A. Curtis, J. Ulrich, A. Montaser, J. M. Prausnitz, and H. W. Blanch, "Protein-protein interactions in concentrated electrolyte solutions - Hofmeister-series effects", *Biotechnology and Bioengineering* **79**(4), pp. 367–380 (2002).

Attached Publications